Modified Titanium Surfaces for Biomedical Applications: Preparation, Physico-Chemical Characterization and Biological *in vitro* Evaluation

February 23, 2009

Chonbuk National University Graduate School

Department of Bionanosystem Engineering

By

Madhav Prasad Neupane

Modified Titanium Surfaces for Biomedical Applications: Preparation, Physico-Chemical Characterization and Biological *in vitro* Evaluation

By

Madhav Prasad Neupane

A Dissertation submitted to the faculty of Chonbuk National University in partial fulfillment for the requirements for the degree of

Doctor of Philosophy

Department of Bionanosystem Engineering

Under the Supervision of Professor Min Ho Lee

September 24, 2008

This thesis is examined and approved for the doctorate degree

Chairman	Chonbuk National University	Prof. Tae Sung Bae
Vice Chairman	Chonbuk National University	Prof. Ho Keun Yi
Member	Chonbuk National University	Prof. Seong Kyu Han
Member	Chonbuk National University	Prof. Jae Gyu Jeon
Member	Chonbuk National University	Prof. Min Ho Lee

December 15, 2008

Chonbuk National University Graduate School

DEDICATION

I would like to dedicate this dissertation to my father Toya Nath Neupane, mother Guna Maya Neupane, wife Apshara Neupane, and beloved daughter Asma Neupane. Without their encouragement and support, this doctorate degree would not have been possible.

Table of Contents

I I

IV. Fabrication of titanium oxide nanotubes by electrochemical anodization in acidic fluoride solution: Study the phase transformation and stability

V. The electrochemical behavior and characterization of the anodic oxide film formed on titanium in phosphate buffer media with different pH

List of Tables

List of Figures

Modified Titanium Surfaces for Biomedical Applications: Preparation, Physico-Chemical Characterization and Biological *in vitro* Evaluation

Madhav Prasad Neupane
Department of Bionanosystem Engineering
Graduate School
Chonbuk National University

Abstract

Metallic titanium and its alloys have become key materials for biomedical applications, mainly owing to their compatibility with human tissues and their mechanical strength. They are used as implant materials such as dental implants and various orthopedic and osteosynthesis systems in contact with bone. Titanium covered with a passive oxide film, is a rather bioinert material. Titanium and its alloys have high enough strength and toughness to bear loads. In order to obtain the favorable properties of titanium metal as implantation, titanium surfaces are modified with different methods. A number of different surface modification methods have been invented and developed; of which

many suffer from low durability and relatively low adhesion of coating on the metal substrate.

This thesis deals with the modification of pure titanium surface by different methods anodic oxidation, quenching, and cyclic voltammetry to obtain favorable properties of titanium surface with improved coating integrity and adhesion. The resulting modified surfaces were characterized using Scanning Electron Microscopy (SEM), Energy Dispersive X-ray Spectrometer (EDS), X-ray Diffraction (XRD), and surface roughness test by using Surftest Formtracer. Also after modifying the titanium surfaces the biological *in vitro* evaluation was performed. Chapter I of this thesis highlights literature overview of history and types of methods of surface modification of titanium, applications, and effects of surface characteristics on biological responses with modified surfaces. Remaining chapters demonstrate the modification, characterization and their potential applications in *in vitro* biological evaluation. Chapter II highlights the control quenching of titanium metal to obtain metal products having particular surface properties. Quenching of metal also relive the internal stresses of metal. This chapter focuses on surface topography, roughness, crystallite size, and crystal intensity of quenched surface with heating temperature. Cytotoxicity of the quenched surface was evaluated with MTT assay. The surface roughness and crystallite size was increased and cytotoxicity of quenched surface was decreased as the heating temperature increased. Similarly, crystalline intensity was varied at different temperature. In chapter III, micro-arc oxidation (MAO) surface modification method is evaluated as a technique to obtain the favorable properties of titanium with

improved coating integrity and adhesion. MAO, an advanced anodization method, allows for anodic oxide layer formation and incorporation of P ions from electrolyte in one single process step. The method exploits the dielectric breakdown of anodic oxide film at high electrical field strength to produce a porous oxide layer with a thickness of a few micrometers that contains different amounts of P ions. A major advantage is the interfacial integrity as a result of the electrochemical reaction between titanium metal and electrolyte. Additionally, MAO is a fast single-step process that is less expensive and much more suited to coat implants than other deposition process such as plasma spraying.

This chapter focuses on two main topics:

● The investigation of the MAO surface modification process, also known as anodic spark deposition, interms of process mechanism and the influence of process parameter “electrolyte pH” on the resulting MAO coating properties.

● The development of bioactive coating consisting of a phosphated titanium oxide matrix that facilitates possible growth of hydroxyapatite as well as osteoblast response.

Firstly, the influence of the process parameter “electrolyte pH” on the dielectric breakdown properties, the coating structure, crystallinity, and chemical composition were investigated by using phosphate buffer electrolyte. The resulting coatings were characterized using SEM, EDS, XRD and surface roughness test. It was illustrated that the parameter “electrolyte pH” influences the surface topography, crystallinity, and surface roughness of modified surface. Secondly, the phosphate buffer electrolyte with different pH was found to

incorporate P ions in MAO coatings with different quantity. A cell-culture study was carried out with MC3T3 mouse osteoblasts in order to test the biocompatibility of the coating with different pH modified surfaces in comparison to uncoated CP titanium surfaces. The results indicated that the MAO coatings are not less biocompatible than the commercially available implant surfaces with respect to cell growth and cytotoxicity evaluation. Finally, the MAO process was investigated by means of a high-resolution SEM to study the mechanism of film formation. Chapter IV deals the formation of titanium oxide nanotubes in acidic fluoride solution by anodic oxidation. After the formation of nanotubes its stability and crystal phase transition was studied at different temperatures. Finally, formation model of titanium oxide nanotube was proposed. At the end, chapter V demonstrates the corrosion of titanium metal at different electrolyte pH. Also the numbers of potentiodynamic cycles were applied on previously formed oxide film. The corrosion of metal linearly depends on electrolyte pH as well as number of potentiodynamic cycles.

In summary, the thesis will direct the idea of different surface modification methods, which can provide a better method as compared to either one method. And it also appreciates to use those modified implant materials that comes from the different modification methods would be the best candidate in the future for dental and orthopedic implant.

Keywords: Anodization, Cell viability, Microstructure, Bioactivity, Osteoblast, Quenching, Biocompatibility, Cell proliferation, Titanium dioxide, Nanotube, Anodic oxidation, Rutile, Anodic oxide, Corrosion, Osseointegration.

I. Literature Review

1. Introduction

Metals have been successfully used as implants in the human body for at least two thousand years, when ancient civilizations used gold for dental purposes [1]. Since first being developed to treat diseased teeth in the ancient world, the purpose and size of implants has dramatically changed [1]. As our knowledge of the human body, the immune system, and toxicology has increased, so has the realization that the metal implants used in the human body are not as unreactive as once believed. Implants that were once considered inert and the destruction of surrounding bone cells [2-4], along with particulate formation caused by fretting [5]. Some of the engineering materials presently used for implants include stainless steels, Co-based alloys, Ti, Ta, Pt and Ir metals. Titanium was first introduced into the medical field in the early 1940s with the publication of an article by Bothe, Beaton and Davenport [6] on the reaction of bone to multiple metallic implants. But commercial usage of titanium as an implant began in the 1960s, despite the fact that it exhibits superior corrosion resistance and tissue acceptance when compared with stainless steels and Cr-Co alloys.

1. 1. Titanium and titanium oxides

William Gregor discovered titanium in 1791 in England, and began to be used practically in 1948 when its commercial production started in the United States. Titanium is a lightweight and strong material with a tensile strength comparable to carbon steels, and because the Young's modulus of titanium is only a half of carbon steel, titanium is soft and readily formed, with spring back

greater than carbon steel's. Titanium is classified in two categories: commercially pure titanium (Ti) which is used in the chemical process industries and titanium alloys having such additives as aluminum (Al) and vanadium (V) and which are used for jet aircraft engines, airframes and other components. Also, unalloyed and alloyed titanium have been used in medical engineering. Further more, according to the content of oxygen, commercially pure titanium was classified into four grades, with grade 4 having the most (0.4%) and grade 1 the least (0.15%) [7]. The quality of different grades Ti with typical impurity contents and their influence in physical and chemical properties are shown in table 1.

Quality	Impurity Contents (%)				Description
	O	N	C	Fe	
High purity - Ti					High purity Ti has one half the oxygen content as commercially pure (ASTM grade 1) titanium. High purity Ti is produced from special grade of sponge(< 0.1 wt% oxygen)
ASTM Grade 1	0.15	0.05	0.10	0.20	Grade 1 has the highest purity, lowest strength, and the best room temperature ductility and formability of the four ASTM unalloyed Ti grades
ASTM Grade 2	0.25	0.03	0.10	0.30	ASTM grade 2 Ti is the workhorse for industrial applications requiring good ductility and corrosion resistance. The guaranteed minimum yield strength of 275 MPa for grade 2 is comparable to those of annealed austentic stainless steels.
ASTM Grade 3	0.35	0.05	0.10	0.30	Like the other grades of Ti metals and alloys, grade 3 bridges the design gap between aluminium and steel, grade 3 has lower iron limits than grade 4 Ti.
ASTM Grade 4	0.40	0.05	0.10	0. 50	Grade 4 has the highest strength of the four ASTM grades of unalloyed Ti and outstanding corrosion fatigue resistance in salt water, but also moderate formability.

Table 1. Different grades of quality of cp Ti together with the corresponding typical impurity contents (wt %) and their influences on the physical and chemical properties

Ref: M. A. Imam, and A.C. Fraker; in: Medical applications of titanium and its alloys: The Material and Biology Issues, edited by S.A. Brown and J.E. Lemons, ASTM STP1272 (1996) 3-14.

Titanium is a successful biocompatible material that is extensively used for biomedical applications, especially for bone-anchoring systems such as joint replacement parts, bone fixation materials, dental implants, heart pacemaker housings, artificial heart valves, surgical instruments, cardiovascular devices, external prostheses etc. It has advantageous bulk

mechanical properties such as a low modulus of elasticity, a high strength to weight ratio, and passive surface properties i.e. excellent corrosion resistance and low rates of ion release as well as a high degree of biocompatibility which is largely attributed to an inert surface oxide film [8, 9]. Since 1960s, dental implants have been used as an artificial anchoring of dentistry in the maxilla and mandible. Titanium and its alloys were commonly used to make up implants because of their optimal physical characteristics and biocompatibility. The physical properties of pure titanium are given in following table 2. Good osseointegration should be essentially formed at the interface between implant surface and living bone during healing procedure after implantation surgery [10]. Surface properties of the implant may play a very important role in immediate reactions on the implant surface after exposure to the tissue and influence the initial processes of osseointegration, which are conceivably important for the clinical success of the implantation. During the past decades, many surface modifications, such as coating, abrasion, blasting, acid etching, oxidation, or combinations of these techniques, were proposed to improve the biocompatibility of the implant surface by altering surface topographies, physical characteristics and chemical properties of titanium.

Properties	Description or Values
Atomic number	22
Atomic weight	47.90
Atomic volume	10.6 W/D
Crystal structure	
Alpha, hexagonal, closely packed (≤882.5ºC)	
c (Å)	4.6832 ± 0.0004
a (Å)	2.9504 ± 0.0004
Beta, cubic, body-centered (≥882.5ºC)	
a (Å)	3.28 ± 0.003
Colour	Dark gray
Density	4.54 g/ cm^3
Melting point	1668 ± 10ºC
Solidus/ Liquidus	1725ºC
Boiling point	3260ºC
Thermal conductivity	19.2 W/ m K
Tensile strength	240 MPa
Young's modulus	120 GPa
Poisson's ratio	0.361
Electrical resistivity (at 20ºC)	
High purity	42 μΩ cm
Commercial purity	55 μΩ cm
Temperature coefficient of electrical resistance	0.0026/ ºC

Table 2. Summary of physical properties of pure titanium

In different surface modification methods, titanium forms a thin oxide layer approximately 2 to 10 nm thick spontaneously in air, which provides corrosion resistance [11-13]. The electronic structure of titanium consists of $1s^2$, $2s^2$, $2p^6$, $3s^2$, $3p^6$, $3d^2$, $4s^2$ in which the lightly held $3d^2$ and $4s^2$ electrons are highly reactive, and thus titanium can spontaneously and instantaneously form

a tenacious oxide, which varies both thickness and composition under certain circumstances. As the titanium is in contact with host tissues, it interacts with physiological fluids through its oxide film, which is responsible for corrosion resistance and biocompatibility [14, 15]. Both thickness and chemical composition of titanium oxide layers may play an important role in adsorption of proteins from physiological fluids and attracting cells to its surface. By using thermal or electrochemical oxidation treatments, much thicker oxides can be produced [16, 17]. The surface oxide film has several oxides (TiO_2, TiO, Ti_2O_3) and among them TiO_2, the most common, is probably the most stable. TiO_2 exists as three crystalline forms including the orthorhombic brookite, the tetragonal anatase and rutile. In most cases, the main chemical composition of titanium oxides is TiO_2, however, electrochemically prepared oxides may also contain some impurities due to ion incorporation from the electrolytes used, such as Cl, S, Si, P, Ca, and Na [11, 12]. When exposed to air or to biologic fluids, the titanium oxide layer is easily contaminated by hydrocarbons or other elements, for the TiO_2-terminated surface tends to bind molecules or atoms from the surroundings as a monomolecular layer [18].

1. 2. Titanium surfaces and their modifications

The stability of an implant is determined by their osseointegration, which in large part depends on the chemistry and topography of its surface. Although the surface oxide film on titanium can be healed by itself within milliseconds, the dissolution of metal ions during its regeneration into the human body can induce the release of potentially osteolytic cytokines involved in the implant

loosening [19]. Besides, the healing process of the interface between titanium and hard tissues, or osseointegration, is slower and the fixation of the titanium implant with host tissues is rather weak. Surface modification can alter the surface topography, chemistry and surface energy which directly determine the implant-environment interactions after implantation. Many attempts have been made to improve the surface properties of titanium-based implants. A number of surface modifications and strategies have been developed to improve the osseointegration of titanium implants and can be divided into physical and chemical treatments as well as a combination of both.

1. 2. 1. Why modifying titanium implant surfaces?

The purpose of surface modification is to retain the key bulk properties of the material while modifying the surface to improve biocompatibility. Typically, modifications can either alter the atoms, compounds, or molecules on the existing surface chemically or physically, or coating the existing surface with a different material. In this section, some of the important surface modifications are discussed, with a great deal of emphasis on coating and texturing operations.

1. 2. 2. Physical Methods

Some physical modifications of the titanium surface only affect its physical characteristics, such as roughness, microtopography, or wettability, and the alterations of all these characteristics may affect the osteoblasts response to modified titanium surfaces directly or indirectly. Machined, sandblasted, and titanium plasma-sprayed titanium have been already tested *in*

vitro by many authors [20-22], and these methods have been applied by some manufacturers to produce commercial implant systems as well [23]. The studies from Mustafa et al. showed that surface roughness of modified titanium increased (R_a: the average roughness, increased from 0.2 μm to 1.38 μm) when the size of the TiO_2 particles used for plasma-spray was enlarged (from 63 μm to 300 μm) [21]. In 2002, Shibata et al. used glow discharge plasma (GDP) to modify titanium, and the osteoblast cell culture on titanium with and without GDP modification indicated that GDP promoted cell adhesion and differentiation on Ti by increasing the adsorption of proteins [24]. There are also some treatments, which use physical methods to modify the chemical composition of the titanium surfaces, such as ion implantation, physical vapor deposition nitriding, and plasma ion nitriding [25-28]. Thermal oxidization can form an outer "ceramic" layer of rutile on titanium alloy [29]. Feng et al., in 2003, reported that thermal treatment of titanium in a different atmosphere could alter surface chemical composition, surface roughness, surface energy, and furthermore improve osteoblast responses to modified titanium surfaces [30]. In this thesis, simple quenching method is evaluated as a physical method to accomplish the favorable properties of titanium and also improve MC3T3 osteoblast responses to quenched titanium surface.

1. 2. 3. Chemical Methods

It is well known that chemical compositions of titanium surfaces are important for protein adsorption from biological fluids and cell response to titanium. Feng et al. compared osteoblastic cells responses to three different titanium surfaces containing calcium, phosphate ions, and carbonate apatite,

respectively, and demonstrated that calcium ions on titanium surfaces play a more important role than phosphate ions in influencing initial interactions between cell culture medium, osteoblasts and titanium [31]. It has been reported that titanium surfaces are easily contaminated by some elements from air, such as C and N, and contamination of titanium surfaces can affect its biocompatibility [32]. Some chemical treatments have been used to reduce the contamination of C and N [33].

Acid etching and hydroxyapatite deposition are the most commonly used chemical treatments. Using HNO_3 or a mixture of HNO_3 and HF to prepare titanium specimens has also been reported in the literature. However, the concentrations of used acids were different between authors, for instance, Bowers and co-workers, in 1992, used a mixture of 25% HNO_3 and 3.5% HF, while a mixture containing 52% HNO_3 and 10% HF was used by Degasne et al. in 1999 [22, 34]. Other inorganic acids, such as HCl, H_2SO_4, and H_3PO_4 were also used to modify the titanium surface or reduce its contamination with other elements [31, 35]. It has been reported that HCl/acetone treatment is an excellent decontamination method for the surface preparation process of Ti [33]. Viornery et al, in 2002, investigated osteoblast cultures on polished titanium disks modified with phosphonic acid. There was no statistically significant difference concerning cell proliferation and differentiation between phosphonic acid modified titanium and unmodified titanium, however, the synthesis of total amount of proteins and collagen type I was significantly higher on the titanium modified with ethane - 1, 1, 2 - triphosphonic acid than unmodified titanium [36].

Hydroxyapatite is a major component and an essential ingredient of normal bone and teeth, and has been widely used as an artificial refill biomaterial for plastic surgery and dental implant. For dental implant applications, plasma-spray, sol-gel, and sputtering techniques were used to produce hydroxyapatite coatings on titanium [37-41]. However, some drawbacks of hydroxyapatite coatings on titanium produced by plasma-spray have been announced: resorption of coating, poor mechanical properties, high thickness, non-homogeneity, lack of adherence [42]. Pulsed laser ablation was used in 2001 as a new method for deposition of a thin layer of hydroxyapatite on titanium surfaces [43]. In the study, the authors used three different laser fluences: 3, 6, and 9 J/cm^2 to deposit the hydroxyapatite layer, and they found that the cell response to the treated surfaces correlated with laser fluences used. Hydroxyapatite coated implants have been produced also by ion beam assisted deposition [44-46]. Recently, hydrothermal treatment after anodic oxidation of titanium has been reported to be able to form thin hydroxyapatite coatings [47-50]. Since dissolution of hydroxyapatite occurs when it is immersed in extracellular fluids at low pH, other alternative apatites, such as fluorapatite and fluorhydroxyapatite, were used to form coatings with strong resistance against degradation [51, 52]. Protein adsorption from serum to biomaterial surfaces is considered as the initial step of osseointegration happening between bone and implant. It has been proven that some proteins, like fibronectin or vitronectin, which adsorb onto biomaterials surfaces when they make contact with biological fluids, can improve cell adhesion [34]. It was indicated that RGD peptides regulated the spreading of HOS cells on hydroxyapatite but not

on titanium surfaces, and the spreading of osteoblasts mediated by the RGD domain of vitronectin and fibronectin might contribute to the oseoconductive ability of hydroxyapatite [53, 54]. The studies from Tossati and co-workers, in 2003, have shown that peptides of RGD (Arg-Gly-Asp) and RDG (Arg-Asp-Gly) type functionalized poly (L-lysine)-grafted-poly (ethylene glycol) (PLL-g-PEG) copolymers grafted onto titanium surface can resist non-specific protein adsorption onto its modified surface. Therefore, peptide-functionalized PEG may elicit specific interactions with integrin-type cell receptors in the presence of full blood plasma [55]. A coating of 91.2% de-acetylated chitosan on titanium decreased its wettability, but increased protein adsorption and cell attachment [56].

1. 2. 4. Combination Methods

Combinations of physical and chemical methods can alter both physical properties and chemical compositions of titanium surfaces at the same time, or create a more intensive modification than using only one technique. The SLA (sandblasted with large grit and acid etched) surface has been documented to lead to a rapid and strong implant fixation *in vivo* [57-59]. An electropolishing technique was carried out in an electrolyte consisting of 540 ml methanol, 350 ml n-butanol and 60 ml perchloric acid, held at – 30^{o}C for 5 min with the voltage of 22.5 V. A very smooth mirror-like titanium surface with the oxide thickness of 4-5 nm could be produced with this method [60]. Another commonly used combination method is anodic oxidation, which is a similar procedure to electropolishing, but the electrolyte composition and process

parameters, such as temperature, voltage and current, in the electrochemical cell should be changed.

1. 2. 4. 1. Anodic oxidation on commercial pure titanium

An electrochemical method known as anodization or anodic oxidation is a well-established surface modification technique for valve metals to produce protective layers. Anodic oxidation on commercial pure titanium has been used to improve the biocompatibility of titanium [47-49, 60-64]. Anodic oxidation is a combination of physical and chemical processes for increasing oxide thickness and altering properties of the titanium surface. The general principle of this technique is the application of an electrical charge to the specimen in an electrolyte solution. The characteristics of the resultant anodic oxide film, such as surface roughness, microstructure and composition, may be influenced by the following anodic oxidation parameters: applied voltage, current density, electrolyte temperature, pH, and the components and concentrations of electrolyte solutions [63-66]. Larsson et al. used 1M acetic acid as an electrolyte to anodize titanium implants [60]. Ishizawa and Ogino found that sodium β-glycerophosphate (β-GP) and calcium acetate (CA) were suitable for the electrolytes to form an anodic titanium oxide film containing Ca and P (AOFCP) on commercially pure titanium [47-49]. And the formed oxide films in these electrolytic solutions have a Ca/P ratio equivalent to hydroxyapatite (HA, Ca/P ratio is 1.67). However, no calcium phosphate peak was detected by X-ray diffraction (XRD), and the AOFCP consisted of anatase and only a little rutile. The thickness of the AOFCP produced at 350 V was about 10 μm. Further more; the formed AOFCP had a high adhesive strength to titanium after

soaking in a simulated body fluid for 30 days. Zhu et al. produced a titanium oxide film enriched with Ca and P in alternative electrolytes of calcium glycerophosphate (Ca-GP) and calcium acetate (CA) by galvanostatic mode [67]. Under different conditions, i.e., different concentrations of electrolyte, current density and sparking voltages, the range of roughness (R_a) of the formed film was 0.37 – 0.98 μm, Ca/P 0.46-1.69, and the thickness were also increased up to 5-7 μm. In contrast to the oxide films formed in the electrolyte of β-glycerophosphate sodium and calcium acetate, for which it has been reported that some microcracks were observed on the formed film [62], no microcrack was found on all the oxide films anodized in the electrolyte of Ca-GP and CA. Other alternative electrolytes, such as sulphuric acid and phosphoric acid with or without calcium compounds, were used as well [50, 63, 64]. The optimal biocompatibility of titanium is due to the most part to oxide layers spontaneously or passively formed on titanium surface. The oxide layers contact directly the cell culture medium *in vitro* or surrounding living tissues *in vivo*, and physical or chemical reactions will happen on these interfaces. It has been reported that metallic ions were released from metallic implants into the surrounding tissue *in vivo*, which may cause acute inflammation without evidence of bacterial infection, allergic reactions and malignant disease [68-72]. The corrosion-resistance of titanium oxide films can be greatly improved by anodic oxidation [73]. Anodic oxidation can apparently increase the thickness and stability of oxide layers on titanium, and consequently improve the resistance against release of titanium ions. Kanematu et al., in 1990, produced an oxide-anodized titanium alloy (TiO_2/Ti-6Al-4V) with a 138 nm thick layer

of titanium oxide compared to the basic titanium alloy with a 1-1.5 nm thick oxide layer, and with decreased titanium ion dissolution [61]. Larsson et al. anodized titanium in 1M acetic acid at room temperature and using two different voltages, 10 V and 80 V. Because of the low anodization voltages, thin oxide films were formed 21 nm and 180 nm thick, respectively [60]. However, other authors produced much thicker oxide films with alternative anodizing methods and electrolytes [47-49, 62-64], and the thickness of oxide layers can be up to 10 μm. Since good interaction between implant and bone tissue and enhanced osseointegration are essential for a successful implant, substantial efforts were made to test the bone tissue responses to anodized titanium *in vivo* [60, 63, 74].

Larsson et al. inserted machined titanium implants, electropolished titanium implants and the anodized implants prepared in 1M acetic acid with 10 V and 80 V voltages into proximal tibial metaphysis of adult New Zealand white rabbits, and the machined implants were used as controls. After 7 weeks, the results demonstrated that the highest bone contact was found for the implants with a thick oxide (80V anodization) and the lowest values for the electropolished implants [60]. Y. T. Sul and co-workers [63] prepared implants with 0.2-1 μm thick oxide films surfaces with an average roughness of 0.96-1.03 μm, and the implants were inserted into rabbit tibiae for six weeks. The results showed that implants with an oxide thickness of approximately 600, 800 and 1000 nm demonstrated significantly higher removal torque values than the implants with thinner oxide films, approximately 17 and 200 nm. However, no significant difference between implants with oxide thickness of 17 and 200 nm

was detected. Therefore, oxide thickness of implants may play a critical role in bone tissue response to implants. However, it is not fully understood whether these oxide properties influence the bone tissue response separately or synergistically. Son et al. [74] investigated the bone response to anodized titanium or titanium treated by anodization followed by hydrothermal treatments *in vivo*, and used untreated titanium as control. The removal torque strength was significantly higher for anodized implants than for the untreated implants at 6 weeks after implantation in a rabbit model, although there was no significant difference concerning bone contact on all implants. Although surface properties of anodic oxides on titanium have been reported extensively in the literature [47-49, 62-64], and some studies evaluated their biocompatibility *in vivo*, there are little data about the behavior of osteoblastic cells on anodized titanium surfaces *in vitro*. In the present study, anodization in 1M phosphate buffer with different pH is evaluated as a combined method to accomplish the favorable properties of titanium and also improve MC3T3 osteoblast responses to anodized titanium surface.

1. 2. 5. Effects of surface characteristics on biological responses

A variety of surface properties are believed to be responsible for the favourable performance of titanium implants, in particular the presence of a chemically very stable oxide film protecting the underlying metal from corrosion, the moderate charge of the surface under biological conditions, the very low concentration of charged species within the dissolution products and a dielectric constant ε for titanium oxide close to that of water (ε = 78).

1. 2. 5. 1. Surface energy

The interaction between the outermost surface of a biomaterial and its environment is a highly dynamic process, in which protein adsorption is a key factor. Surface energy, initially, may play a major role in determining which proteins are adsorbed onto the surface, as well as whether or not the cells themselves adhere to the surface, and further influences the latter stage of bone formation and calcification through preferring the adhesion of some cell types [75]. Wettability, a measurement of surface energy, is often used as one of surface characteristics. Normally, the amount of adsorbed protein is higher on hydrophobic surfaces than on hydrophilic surfaces [76, 77]. However, strong hydrophobic, low-energy materials, e.g. polydimethysiloxane-pretreated surfaces, exhibited a low tendency to adsorb proteins due to energetically unfavorable conditions [78], and strong hydrophilic materials suppressed the protein film adsorption, probably due to the absence of both hydrophobic interactions and double-layer attraction forces [79], as protein adsorption depends on the magnitude of the interacting forces between the biomolecule and the surface. Cell adhesion, different from protein adsorption, occurs readily to hydrophilic surfaces but inefficiently to hydrophobic surfaces. Generally, surface energy is proportional to cellular adhesion strength, and thus, the metals of high energy have much greater adhesion strength of cells than the polymeric materials of lower energy. The clean titanium surface is hydrophilic due to the high polarity of the Ti-O bond and its surface contamination such as carbon or hydrocarbon adsorption produces high values of water contact angles. Surface energy can readily be changed by processing in the preparation of titanium

implants. By glow charge, increased surface energy results in the increase of cellular adhesion [80]. Osteoclast differentiation is greatly activated by glow charge pretreatment [81]. Increased surface energy does not selectively increase the adhesion of particular cells or tissues, and it has not been shown to increase bone-implant interfacial strength [82]. By inserted in the rabbit tibia and femur, glow-discharge-treated implants demonstrated similar early bone healing responses to those with the conventional implant treatment [83]. As the surface of the material is more or less inhomogeneous, surface energy alone is not enough to display the surface characteristics and postulate the interaction of cells and surfaces. On the other hand, surface energy is dictated by surface composition and topography (including roughness) of the implant.

1. 2. 5. 2. Surface topography

The response of cells and tissues at implant interfaces can be affected by surface topography on a macroscopic as well as a microscopic level. On the cell level, surface topography plays a fundamental role in regulating cell behavior, e.g. the morphology, orientation and adhesion, proliferation and differentiation of mammalian cells [84]. The reactions of cells to topography of the substratum to which they are attached is one of the first phenomena observed in tissue culture and therefore play a major role in the evolution and the properties of the implant-tissue interface, e.g. osseointegration.

(i) Surface roughness

The titanium implant surface can be generally considered to be smooth and rough in terms of its roughness, i.e. the former average surface roughness $R_a \leq 1$ μm while the latter $R_a > 1$ μm. Besides, Wennerberg et al. [85]

suggested that roughness be described as smooth for abutments, whereas minimally rough for roughness 0.5 to 1 μm, intermediately rough for 1 to 2 μm, and rough for 2 to 3 μm. Cell responses to titanium surface characteristics have been shown to vary with cell types as well as cell maturation states. From *in vitro* to *in vivo* studies, a common agreement that greater initial cell attachment of osteoblasts on rough surfaces on titanium is accepted as the amount of roughness is within the dimension of individual cells [86, 87]. In contrast, more epithelial cells and fibroblasts were attached to the smoother surfaces than the rougher ones, and also the proliferation of these cells increased on the smoother surfaces [88]. By culturing rat calvarial cells on titanium surfaces in a range of R_a from 0.14 to 1.15 μm, the maximal attachment was demonstrated on the surfaces with a R_a of 0.87 μm [86]. The effect of surface roughness on cell adhesion probably results from the fact that rough surfaces may adsorb more fibronectin, which, a cell adhesion protein present in serum, can mediate cell attachment and spreading on artificial substrates by interacting with glycosaminoglycans and the cytoskeleton [89], than smooth surfaces [90], preserving the synthesis of extracellular matrix proteins [90]. Morphology of cells varies considerably as surface roughness increases [91]. Cells on the smooth surfaces displayed flat, well-spread morphology synthesized a collagen-rich matrix; while the cells on the rough ones assumed a round or cuboidal shape with cytoplasmic extensions communicating between cells or anchoring the cells to the peaks of the surfaces, and produced collagen based matrix. The morphology of osteoblasts is related to their focal contacts, which distribute uniformly on all the membrane surfaces in contact with the

substratum on smooth surfaces and visible only at the extremities of cell extensions where cell membranes are in contact with the substrate [92]. More cell spreading and continuous cell layer formation were shown on smooth surfaces compared to rough ones [92]. From chondrocytes on the same titanium surfaces, the effect of surface roughness on their proliferation is dependent on the maturation state of the cells [93]. The response of the less mature resting zone cells was comparable to that of MG63 cells, which is postulated to represent a relatively immature osteoblastic state. The more mature growth zone chondrocytes also exhibited decreased proliferation on rough surfaces. Using MG63 cells, Martin et al. [94] demonstrated cells cultured on rougher titanium surfaces exhibited decreased cellular proliferation and expressed more differentiated phenotype, which is a more osteoblastic phenotype. Besides, cells on the rougher surfaces were found to release higher levels of prostaglandin E2 (PGE2) and latent transforming growth factor β (LTGF β) [95], both factors involved in regulation of bone formation. However, some researchers showed osteoblastic proliferation could be enhanced on rough surfaces. All these contradictory data may be ascribed to the sensitivity of cells to the surface features, which are not sufficiently described by surface roughness, implying that implant surface roughness modulates osteoblastic proliferation, differentiation, and matrix production *in vitro*.

In *in vivo* studies, a morphometric analysis showed increasing implant surface roughness generally correlated with increased surface coverage by bone. By evaluating different variables, Thomas and Cook [96] found that surface texture, i.e. a combination of topography and roughness, more than anything

else, significantly affected the interface response to the implant. An implant with a rough surface yielded both greater shear strengths and direct bone apposition, whereas the implant with smooth surfaces exhibited various degrees of fibrous encapsulation. Therefore, rough surfaces are assumed to produce better bone fixation than smooth surfaces. It has been indicated that soft tissues interact better with smooth polished titanium surfaces, whereas rough titanium surfaces rather promote bone tissue formation and osseointegration [97]. On the other hand, an *in vivo* study showed that very different rough surfaces of titanium exhibited a similar bony reaction and no significant difference in the interface length percentage covered by bone [98]. Thus, the organization of surface features also takes effect on bone formation at the implant-implant interface.

(ii) Surface structures

All anchorage-dependent cells, either *in vitro* or *in vivo*, have to contend with some substrate topography. Thus, reactions of cells to topographic cues are important for diverse processes *in vivo* e.g. morphogenesis, cell invasion, repair and regeneration [84]. Cells can discriminate not only between surfaces of different roughness, but also between surfaces even with comparable roughness but different topographies. The micron- and nano-topography can present strong cues for cell behavior and thus, the interactions of cells with topographic features of the substrate they attach to will affect a variety of cellular processes such as cell adhesion, cytoskeletal organization, cell motility, migration patterns and cell differentiation [84, 99, 100]. The reactions of cells to the topography of their substratum, are assumed contact guidance, the

phenomenon has been demonstrated by the organization of surface roughness. The tendency of surface topography to influence cell spreading is called “contact cue guidance” [101]. Such effects depend on not only the size and structures of the features of the substratum but also the cell type. Curtis et al. [99, 101] have shown that cells align themselves with topographical features such as parallel grooves etched into a biomaterial surface. Certain cells, such as fibroblasts cells responsible for producing extracellular matrix in wound healing and tissue remodeling will migrate along the tracks. Others, for instance macrophages, will remain 'trapped' within the features. Epithelial cells were markedly oriented along the long axis of 10 µm deep grooves on titanium coated implants [102]. On grooved surfaces, cells generally align to the long axis of the grooves [103, 104], and the alignment of cells with structures, e.g. grooves, walls and edges, is often accompanied by the organization of actin and other cytoskeletal elements such as microtubules in an orientation parallel to the structures [105, 106]. The analysis at the molecular level indicated F-actin condensations appeared at topographic discontinuities, often at right angles to groove edges, and some cells were observed to have lamellae and filipodia bending around edges. Among cytoskeletal elements, microtubules were the first element to align to grooves, followed by actin [106]. Bone cells on smooth surfaces were oriented randomly or ignored the surface topography on a 0.5 µm grooved surface and span the width of the groove but they are lined up parallel to the grooves in an end-to-end fashion in 5 µm deep grooves [107]. By culturing rat dermal fibroblasts on micro textured silicone, polystyrene, titanium, or poly-L-lactic acid (PLA) substratum with 1, 2, 5, and 10 µm in

width and 0.5, 1, and 1.5 μm in depth [103, 108, 109], it has been observed that the rate of orientation increased drastically when the grooves were made deeper, and however, the number of cells was not highest in the deepest grooves because the cells bridge the grooves [104]. Consequently, it becomes a common agreement that the depth of grooves is more important than their width in determining cell increasing orientation. If surface structures are far greater in size than cells, their effects on orientation of cells disappear. As the groove/ridge width is reduced to the size of the cells or less, the effects on orientation becomes more marked. As to other structures such as pores, much less attention has been paid than grooves. Cambell and von Recum [109] examined the effects of pore size and hydrophobicity in their study involving a cannine *in vivo* implant model. They found that pore size played a larger role than material hydrophobicity in determining tissue response, with pores of 1-2 μm allowing for direct fibroblast attachment. A positive effect of the surface microstructure (pore diameter of 3-8 μm) on both osteoblast fixation and number has been also demonstrated [110, 111]. One probable explanation for increased cell growth is that a porous microstructure presents a stimulus to an orientated cell development [112]; while another is that porous surfaces have a larger culture surface and thereby a lower cell density than smooth surfaces [113]. However, on the smooth surface the cell proliferation was significantly higher in the early phases due to the faster growth. At later time points, the porous surfaces yield higher proliferation. Although a great amount of work has been investigated into preparation and biological responses of different micron- and nano-structured surfaces [84], not much research have been done

on structured surfaces and their cellular reactions of titanium because it is difficulty to apply structuring technologies to titanium surfaces. Anselme et al. [114] observed improved orientation, adhesion and proliferation of human osteoblasts on titanium surfaces with a microroughness (below the cell size) by a lower level in the organization of topography and by relatively high amplitude of topography. Human osteoblasts displayed oriented in a parallel order on polished surfaces and the orientation was not affected by residual grooves after polishing; while on the sandblasted surfaces the cells never attained confluence and had a stellate shape and cell layer had no particular organization [92]. Keller et al. [112] have shown that the highest level of rat osteoblast cell attachment was obtained with rough, sandblasted Ti-6Al-4V surface compared to grooved ones although their R_a values were identical. The reaction mechanism is probably that the sandblasted surface is highly irregular in morphology with many small flatter-appearing areas of various sizes, so that the sandblasted surface may provide a more available area or for attachment of not only cells, but also the extracellular matrix (or preconditioning protein layer) required by the cells for attachment. Therefore, both surface roughness, R_a values, and micro-morphologic patterns (irregular or regular) affect cellular responses.

The osteoblastic response differs significantly with very small porous surface difference. Stangl et al. [115] investigated cell adhesion of osteoblastic cells on cp Ti implants with a series of porous geometries and they postulated that an increase in surface area was not the deciding regulating factor of cell growth at the bone-implant interface, and the implant microstructure was of

importance. For bony ingrowth, the favorable surface pore sizes are in the range from 10 to 500 μm although a border level of 75 μm has been identified in some studies [116]. Li et al. [113] suggested that a porous surface with pore diameter of 140 μm have maximal bony ingrowth. Homsy [117] described a 300 μm pore size as the most favorable and Pilliar [118] proposed that a minimum pore size of 50 μm be used. Porous diameters of 200-400 μm have long been preferred and it is suggested such diameters produce optimal cell migration, adhesion and cellular proliferation [119]. The size (100 μm) of pores is widely quoted as the border level for pore diameter when considering bony ingrowth in mineralized bone. An increase in the surface area of the porous surface alone is not responsible for an increase in cellular proliferation, cell vitality or cell synthesis capability.

1. 3. Osteoblast response to modified titanium surface

1. 3. 1. Osteoblasts

The term osteoblast (from the Greek words for "bone" and "germ" or embryonic) is a mononucleate cell that is responsible for bone formation. Tomes & de Morgen in 1853 first illustrated the existence of a type of cells intimately associated with newly formed bone [120]. In 1864, the term "osteoblast"was first used by Gegenbaur to refer to the "granular corpuscles found in all developing bone as the active agents of osseous growth". Osteoblasts that originate from osteoprogenitor cells and preosteoblasts play a pivotal role in bone formation. During differentiation of the osteoblastic cell lineage, the preosteoblast expresses transforming growth factor-β (TGF-β), which induces osteoblast cell proliferation [121]. Osteoblasts settle at the

surface of the existing matrix and deposit fresh layers of bone onto it. New bone matrix is secreted by osteoblasts, and osteoid is formed, which consists chiefly of type I collagen and the small portion (10-20%) of embedded osteoblasts. While osteoid is rapidly converted into hard bone matrix by the deposition of calcium phosphate crystals, osteoblasts differentiate into mature bone cells, osteocytes. Although the osteocyte continues to secret new bone matrix around itself, it can't further divide. Besides osteocytes, osteoblasts can also differentiate into the other mature cell type, bone-lining cells. The lining cell is inactive and lacks the ability to secret new bone matrix. However, investigations from Chow and coworkers have shown that these cells can be reactivated into bone producing osteoblasts [122].

Under the light microscope, osteoblasts whose synthetic activity is high are plump and polyhedral, while the cells with low activity are usually flattened. It has been discovered with the electron microscope that the cytoplasm of osteoblasts contains large quantities of rough endoplasmic reticulum (ER) forming typical cisterna together with plentiful ribosomes and a well-developed Golgi apparatus, which necessary cellular organs are corresponding to bone matrix secretion [123]. The principal products of the mature osteoblast are type I collagen (90% of the protein in bone), the bone specific vitamin K-dependent proteins, osteocalcin and matrix Gla protein, the phosphorylated glycoproteins including bone sialoproteins I & II, osteopontin and osteonectin, proteoglycans and alkaline phosphatase. The proliferation and differentiation of osteoblastic cells are regulated by systemic agents and a large number of growth factors and cytokines existing in extracellular matrix (ECM), for instance, the insulin-like

growth factors (IGFs), the transforming growth factors (TGF-α and TGF-β), platelet-derived growth factor (PDGF), fibroblast growth factors (FGFs), bone morphogenetic proteins (BMPs), etc. Correspondingly, there are many sorts of receptors for these factors on the cell membrane of osteoblasts, and binding of these factors to their receptors activates signal transduction pathways that finally lead to nuclear responses.

1. 3. 2. Cytotoxicity

Before using the materials in contact with human body, safety tests cytotoxicity assays are required for all products. Cytotoxicity tests using cell cultures have been accepted as the first step in identifying active compounds and for biosafety testing. The choice of cytotoxicity assay will depend on the agent under study, the nature of the response, and the particular target cell Freshney [124]. Assays can be divided into two major classes: (1) an immediate or short-term response such as an alteration in membrane permeability or a perturbation of a particular metabolic pathway, and (2) long-term survival, either absolute, usually measured by the retention of self-renewal capacity, or survival in altered state, e.g., expressing genetic mutation(s) or malignant transformation. A cellular viability assay, one type of short-term assay, is commonly used to test cytotoxicity of biomaterials. Most viability tests rely on a breakdown in membrane integrity determined by the uptake of a dye to which the cell is normally impermeable; or the release of a dye or isotope normally taken up and retained by viable cells. However, some toxic influences from biomaterials only show their cytotoxicity several hours or even several days later and short-term toxicity may be reversible. Therefore long-

term cytotoxicity assays should be performed to indicate the metabolic or proliferative capacity of cells after rather than during exposure to a toxic influence, or as a supplement to short-term assay.

ISO (the International Organization for Standardization) has established the standard for *in vitro* cytotoxicity tests, i.e., ISO 10993-5. In this standard, three categories of tests are listed: extract test, direct contact test, and indirect contact test. The extract preparation plays a critical role in extract test. In ISO 10993-5, it is required that the ratio between the surface material and the volume of extraction vehicle shall be no more than 6 cm^2/ml and no less than 1.25cm^2/ml. In addition, a positive control and a negative control are necessary to estimate cytotoxicity of biomaterials.

Although it has been demonstrated by many studies that titanium has no cytotoxicity and optimal biocompatibility, and it is a safe implant material when implanted into human body, some reports showed that titanium ions released into the body fluid from titanium implants during application may cause cellular damage. Generally, titanium resisted corrosion in chloride solutions, but in dynamic, protein-rich, oxygenated living tissues in which nitrogen is largely absent, the dissolution of titanium into the tissues surrounding a titanium implant is promoted [61,125]. Any modification methods will change the physical characteristics or chemical compositions of the titanium surface, and furthermore may affect the dynamic mechanisms for titanium ion release or contaminate titanium oxides with some toxic chemical elements or molecules. Therefore, in experiments designed for biocompatibility testing of biomaterials, cytotoxicity assay should be done first of all.

1. 3. 3. Cell attachment and spreading

Cell adhesion is involved in various natural phenomena such as embryogenesis, maintenance of tissue structure, wound healing, immune response, metastasis, and tissue integration of biomaterials. Since cellular attachment, adhesion and spreading belong to the first phase of cell/material interactions, the quality of this phase will influence proliferation and differentiation of cells on biomaterials surfaces. Cell adhesion may be affected by surface characteristics of materials, such as their physical properties, chemical composition, and microtopography.

In general, there are two kinds of cell adhesion, one is cell-cell adhesion, and the other is cell-ECM (extracellular matrix) adhesion. The latter is always studied to investigate biocompatibility of biomaterials. Although there are many surface adhesion proteins involved in cell adhesion, for instance, integrin, selectin, mucin families, and the immunoglobin-cell adhesion molecule family (Ig-CAM) etc, members of the integrin family are the main cellular receptors for the extracellular matrix. It has been reported in Inoue and co-worker's review [126] that there are three types of adhesion structures with different separation between attached cells and substratum. The first type of cell-substratum contact is to the extracellular matrix (ECM) with a gap of 100 nm or more between the cell membrane and the substratum. The second type was named closed contact (CC), a large labile structure, where cells are separated from the substratum by approximately 30 nm. The tightest adhesion units with the separation of 10 to 15 nm between cultured cells and substrate surfaces are named "focal contacts", also called "focal adhesions", where integrins cluster

together to transduce transmembrane signals and link actin filaments to the extracellular matrix. On the internal side of the cell membrane, focal contacts are composed of some associated structural proteins, α-actinin, talin, vinculin, paxillin and tensin. These proteins mediate the signal communication between ECM and cytoskeleton to affect cell behavior. Focal contacts play a critical part in fixing cultured cells on the substrate surfaces, as well as in cell migration on the surfaces. When cells move forward, new focal contacts will be synthesized and old focal contacts must be released. In general, cells with a low motility form strong focal adhesions while motile cells form less of these adhesive structures. In lots of cell culture models, immuno-histochemical focal contacts staining by fluorescence dyes was used to describe cell shapes, even double staining with two or more dyes was involved to show both, focal contacts and cytoskeleton, at the same time. G. Schneider and K. Burridge, in 1994, found that precoating glass coverslips or titanium disks with serum or fibronectin enhanced cell spreading and resulted in the rapid formation of focal contacts and their associated stress fibers, and the effect on the samples precoated with fibronectin was better than on those coated with serum [127]. Cell adhesion to the material surface was considered as one of the most important indexes of the biocompatibility of materials, because osteoblasts contact the surface of implanted biomaterials in very short time when biomaterials are implanted into the host and this process plays a critical role in the formation of osseointegration between implants and tissue. The process of adhesion of cells to the substrate involves multiple steps: (1) adsorption of serum proteins to the substrate; (2) interaction between special receptors on the cell membrane which

combine with the proteins adsorbed onto the substrate; and (3) spreading of cells on the substrate [88].

During the whole adhesion and spreading process, one very important cell behavior is cytoskeleton reorganization. The cytoskeleton is a complex network of protein filaments that extends throughout the cytoplasm. It is a highly dynamic structure that reorganizes continuously as the cell changes shape, divides, and responds to its environment. The cytoskeleton composes of three types of protein filaments-actin filaments, microtubules, and intermediate filaments. Actin filaments are two-stranded helical polymers of the protein actin, with a diameter of 5-9 nm, and they are most highly concentrated in the cortex, just beneath the plasma membrane. The three types of filaments are connected to one another, and coordinated to carry out functions. The cortical actin filament network generally determines the shape and mechanical properties of the plasma membrane, and it is organized into three general types of arrays. Parallel bundles are located in microspikes and filopodia, in which the filaments are oriented with the same polarity and are often closely spaced (10-20 nm apart). In contractile bundles, as found in stress fibers and in the contractile ring, filaments are arranged with opposite polarities, and the distance between filaments is always 30-60 nm. The third type of arrays is a gel-like network, in which the filaments are arranged in a relatively loose, open array with many orthogonal interconnections. At one end stress fibers insert into the plasma membrane at special sites, focal contacts, at the other end they attach to a second focal contact or insert into a meshwork of intermediate filaments that surrounds the cell nucleus.

Rajaraman and coworkers [128] classified cell spreading supported by the assembling of cytoskeleton into 4 stages by scanning electron microscopy: (1) rounded cells with a few filopodia; (2) cells with focal cytoplasmic extensions or lamellipodia; (3) circumferential spreading; (4) cells spread fully and flattened into a polygonal shape.

Proteins and other adsorbable macromolecules containing in modified cell culture medium is immediately adsorbed onto the exposed materials' surfaces; 2 to 5 nm layer forms within the first minute of contact. Albumin, pre albumin and IgG were found to be adsorbed onto the TiO_2 surface in a short time by immunoelectrophoresis, when the TiO_2 powder was equilibrated with serum by shaking. Ellingsen also suggested that calcium ions might act as the intermediate between TiO_2 and the macromolecules in serum [129]. These adsorbed proteins and macromolecules play a very important role in the formation of extracellular matrix and subsequent cell attachment. Fibronectin and vitronectin have shown to be involved in cell attachment and spreading of human osteoblast-like cells, SaOS-2, on titanium surfaces [34, 130].

Acid etched, sandblasted and acid etched titanium disks were compared by cell culture of osteoblast-like cells under different medium conditions: only DMEM culture medium, DMEM culture medium supplemented with fetal calf serum, DMEM culture medium supplemented with fibronectin and vitronectin, and DMEM culture medium containing monoclonal anti-integrin ($\beta 1$, αv). The studies revealed that cell adhesion and spreading were significantly decreased by addition of anti $\beta 1$ or αv integrin monoclonal antibodies to the culture medium. Cells appeared scanty and packed in clusters, when cultured in the

absence of FCS, fibronectin and vitronectin; on the contrary, cells extended completely, when cultured in the medium containing FCS, fibronectin and vitronectin [34].

Bowers et al. reported *in vitro* cellular responses of osteoblast-like cells derived from rat calvarial explants to titanium surfaces with different surface morphologies, with the range of roughness of 0.14 - 1.15 μm. Cell attachment assays were performed at 15 min, 30 min, 60 min and 120 min after cell seeding on samples. No significant difference was found at 15 min among all groups with different surface preparations. However, at 30 min, 60 min, and 120 min, the highest percentage of cell attachment was shown on the rough, irregularly patterned sand-blasted surfaces (R_a = 0.87 μm) [14].

Lumbikanonda and co-workers characterized the responses of neonatal rat osteoblast cells to smooth titanium, titanium dioxide-blasted, titanium plasma-sprayed, and hydroxyapatite plasma-sprayed implants, and found that cells spread most quickly on titanium plasma-sprayed implants at the initial cell culture stage. By means of scanning electron microscopy, attached cells were classified according to stage of attachment, and it was found that cells cultured on the titanium dioxide blasted surface showed no adaptation to surface irregularities, while fully spread cells on the smooth titanium implants were closely adherent to the surface [23].

The experiments from Degasne and co-workers, in 1999, indicated that a high surface roughness was a critical element for cell adhesion [34]. The results of these studies showed that rough surfaces could improve cell adhesion on to biomaterial surfaces, which agreed with some other authors [86, 131].

However, other authors had other opinions. For instance, Mustafa et al. compared cellular attachment to TiO_2-blasted titanium implant material with an average roughness of 0.72 μm, 1.3 μm and 1.38 μm and to turned titanium surfaces with the roughness of 0.2 μm as control. It was found that cellular attachment to the blasted titanium surface 1.3 μm rough was significantly lower than to turned titanium, while there was no significant difference between turned surfaces and blasted surfaces with 0.72 μm or 1.38 μm [21]. A. L. Rosa and M. M. Beloti, in 2003 investigated the effect of titanium surface roughness on the response of human bone marrow cells concerning: cell attachment, proliferation, and differentiation, and found that cell attachment was not affected by surface roughness [132].

1. 3. 4. Cell proliferation and differentiation

An increase in the number of cells as a result of cell growth and cell division is called cell proliferation. To grow into multicellular organs and perform special functions, cell proliferation and differentiation must be conducted. The term 'cell cycle' has been used to describe the behavior of cells as they grow and divide. To facilitate understanding of the cell cycle, the whole cycle was divided into several phases and sub-phases. Four phases, G_1 phase (first gap phase), S phase (synthetic phase), G_2 phase (second gap phase), and M phase (mitosis), respectively, were adopted to demonstrate the cell cycle. By improving adsorption of proteins essential for cell adhesion and secretion of ECM on the biomaterials surfaces, modification of biomaterial surfaces can promote cell proliferation and improve their biocompatibility indirectly.

Besides the four phases of cell cycle mentioned above, there is still a special phase, G_0 phase. When cells are in G_0 phase, they stop continuing to divide, but are still capable of re-entering the cell cycle, i.e., in this stage, cells can perform their physiological functions and from this state they can be trigged into the proliferative phase by an appropriate stimulus. When cells enter the G_0 state, there is no increase in cell number, i.e. no real cell proliferation occurs. Differentiation is generally incompatible with proliferation that is, as differentiation progresses, cell division is reduced and eventually lost, and vice versa. After implants are inserted into bone tissue, during osseointegration preosteoblasts should differentiate into osteoblasts and osteoblasts should differentiate into osteocytes to form bone tissue around inserted implants. Cell proliferation and differentiation can be promoted by modifications of the titanium surface.

Stanford and coworkers [133] prepared cp titanium specimens with 600-grit polished, 1-μm polished, and 50-μm Al oxide sand blasted surfaces. Different sterilization treatments were employed to sterilize prepared cp Ti samples, including ultraviolet light, ethylene oxide, argon plasma-cleaning or routine clinical autoclaving. Osteocalcin, collagen expression, alkaline phosphatase activity and alizarin red calcium assay of rat primary osteoblast-like cells were investigated. The results indicated that osteocalcin and alkaline phosphatase activity, but not collagen expression, was significantly affected by surface roughness when these surfaces were treated by argon plasma-cleaning. On a per-cell basis, levels of the marks of cellular differentiation were highest

on the smooth 1-μm polished surface and lowest on the roughest surfaces for the plasma-cleaned cpTi.

It is generally accepted that several responses of osteoblastic cells can be promoted by roughened, textured and porous surfaces [30]. Degasne and coworkes [34] found that cell proliferation was increased on rough but not on smooth titanium surfaces. However, other authors revealed the contrary results. Martin et al. [94], compared five different Ti surfaces ranked from smoothest to roughest: electropolished disks, disks pretreated with hydrofluoric acid-nitric acid and washed, pretreated disks subsequently fine sandblasted and etched with HCl and H_2SO_4, pretreated disks subsequently coarse sandblasted and etched with HCl and H_2SO_4, and pretreated disks subsequently Ti plasma-sprayed (TPS). The results of cell proliferation demonstrated that significantly more cells were on electropolished surfaces than on plastic used as control, while significantly fewer cells were found on TPS surfaces. Postiglione et al. [20], found that human osteoblast-like cells, SaOS-2, proliferated on smooth titanium surface significantly faster than on sandblasted or titanium plasma-sprayed titanium surfaces. On the contrary, the increase of cellular differentiation, indicated by alkaline phosphatase activity, was detected only on sandblasted and titanium plasma-sprayed titanium surfaces. Other authors reported as well that cell proliferation was inversely related to surface roughness [134].

Macroporous TiO_2 films, which consist of monodisperse, three-dimensional, spherical, interconnected pores with the size of 0.5, 16, and 50 μm, were prepared and human bone-derived cells (HBDC) were cultured on these

surfaces [135]. Higher [^{3}H] thymidine incorporation by the HBDC was observed when they were grown on 0.5- and 16-μm pores compared to the 50-μm pores. However, there was no significant difference of cell proliferation among all three kinds of pore sizes.

The opposite effect of surface roughness on cell proliferation of osteoblast-like cells may attribute to different cell lines used in cell culture or to the differences of roughness ranges. Nevertheless, it is proven that cell proliferation and differentiation can be affected by roughness.

1. 4. Research Objectives

The goal of this thesis is to improve the biocompatibility of alloyed or unalloyed titanium or to achieve a better osseointegration between titanium implant and the bone tissue of the host. Many efforts have been undertaken to modify physical and or chemical characteristics of titanium surfaces. Quenching of pure titanium at different temperatures and anodic oxidation has been used to modify titanium surfaces. Characterization and cell response of modified titanium surfaces will be investigated to understand cell reactions to their structures and chemistry. These modifications should be able to directly control biological response to the titanium (implant) surface.

The main content of the current study includes:

1. Surface characterization and cytotoxicity evaluation on quenched titanium surfaces at various temperatures.

2. Preparation and characterization of anodic titanium oxides at different electrolyte pH incorporated with P and evaluate the cytotoxicity of modified surface.

3. Preparation and characterization of titanium oxide nanotubes in acidic fluoride solution and study the phase transition and stability of nanotubes.
4. Cyclic voltammetry is employed to study the corrosion of pure titanium at different electrolyte pH.

II. Modification of titanium surface by thermal and quenching treatment and its cytotoxicity evaluation

In this study we characterizes the surface of the oxide film that forms on titanium metal through the use of thermal and quenching treatments in cold water and investigates the effects of the surface characteristics and cellular interactions of a modified titanium surface. The as received sample group was prepared by polishing and cleaning cp-Ti as a control group and thermal and quenching sample groups were prepared by heat treating at 600, 700, 800, 900, and 1000^{o}C respectively and subsequent quenching in cold water. The surface topography, roughness, crystallite size and crystal intensity were found to depend on the heating temperature. An increased surface roughness was observed with increases in the heating temperature and the quenching. The surface roughness was in the range of 0.15 μm-1.07 μm. In vitro cell responses were evaluated with mouse osteoblast MC3T3 cells in terms of cell proliferation and differentiation. MTT assays showed an increase in the living cell density and proliferation upon heating and quenching the titanium surface. The results of this study indicate that the cell toxicity was sensitive to the surface roughness and that it decreased as the roughness of the Ti increased.

1. Introduction

Titanium and its alloys are widely used in load bearing dental and orthopedic implants due to attractive properties such as their biocompatibility, corrosion resistance, lightness, durability, high strength, and because they can be prepared in different forms, shapes, and textures [136–139]. As titanium is a very active metal, it reacts with oxygen in the air and forms a dense and stable oxide film with a thickness of a few nanometers. The biocompatibility of titanium and its high corrosion resistance are attributed to this surface oxide film [140, 141]. Titanium is, however, a bioinert metal and is not chemically attached to bone. The bone growth rate on the surface of titanium implants is low compared to that of implant materials coated with calcium phosphate [142–144]. Thus, a considerable number of studies have been conducted to improve the bioactivity of titanium using surface modification methods such as chemical treatments [145–147]; thermal treatments [148]; electrochemical methods [149]; anodization [150]; coating the titanium surface with calcium phosphate or bone morphogenetic protein, which have superior bioactivity compared to natural oxidation film [151–153]; or changing the crystalline structure and morphology of the surface oxide film on the titanium surface using various preparation and oxidation techniques [140, 154–156]. During various surface modification procedures, titanium metal may come into contact with different thermal environments with a range of surface characteristics involving different surface morphologies, crystalline structures, crystallite sizes, and roughness levels. These different surface characteristics are important factors related to bioactivity and cellular interactions.

In earlier studies, the anatase structure was observed in TiO_2 prepared by a sol-gel method or by anodization at low temperatures [157–159], while titanium oxide of a rutile structure was it typically shown to form by a thermal treatment [155, 156, 160]. It has been reported that the crystalline structure of titanium oxide film is dependent on the method of oxide formation, the type of substrate, and the surface conditions [161]. In addition, it has been reported that the contents of a hydroxyl group that existed on a titanium surface oxide film played an important role in the improvement of bone growth as this group acted as a nucleus for the creation of apatite [141]. The OH^- groups on the oxide surface also increase the hydrophilic property of the surface, which enhances the cell growth. Changes in the crystalline structure and in the contents of the OH^- groups on a modified titanium surface have been reported in many articles. Studies that are more systematic are required to endorse the effects of the changes of the topography, crystalline structure, and surface roughness induced by thermal treatments on the bioactivity and cellular interactions. Titanium metal heated to high temperatures above 700^oC in air is difficult to use as an implant because the adhesion between the oxide layer and the substrate rapidly decreases [162]. However, discussion of the effects of the surface characteristics of titanium oxide formed by a high-temperature thermal treatment and subsequent quenching on the bioactivity may provide information regarding the satisfactory surface condition for a titanium implant.

This work aims to study the surface characteristics of a quenched titanium surface and bone cell material interactions on a pure titanium metal surface that has been modified via thermal treatment and quenching in ice cold water.

Titanium oxide layer were grown on titanium surfaces by quenching. The biological properties of these surfaces were evaluated *in vitro* in terms of the behavior of osteoblast cells cultured on the quenched titanium surface and the effect of this structure on the morphology of osteoblast cells was investigated. Also investigated was the kinetics of cell proliferation. Such accelerated cell growth is beneficial for faster healing of dental and orthopedic patients. It can also be used with a variety of biomedical diagnostic and therapeutic applications.

2. Materials and methods

2. 1. Materials preparation

Commercially pure titanium (Grade 2) sample that measured 20mm × 10mm × 2mm were degreased with acetone, polished with #220 to #800 SiC papers and ultrasonically cleaned in distilled water and ethanol. Different samples of the cleaned plates were isothermally heated (5^{o}C /min) to 600^{o}C, 700^{o}C, 800^{o}C, 900^{o}C and 1000^{o}C under normal atmospheric conditions for 2 h and were then rapidly quenched in ice cold water to relieve internal stress [163, 164].

2. 2. Surface characterization technique

The surface micro-morphologies of the sample groups were observed using a scanning electron microscope (SEM) (JEOL JSM-5900, Japan) connected to an energy dispersive X-ray spectrometer (EDS). The crystalline structure was identified via X-ray diffraction (XRD) (Dmax III-A type, Rigaku Co., Japan) using Cu Kα incident radiation, a tube voltage of 40 kV and a current of 30 mA. The scanning angle ranged from 20^{o} to 60^{o} 2θ with a

scanning rate 4^{o}/min. The surface roughness of the specimens was quantified using a Surftest Formtracer (Surftest SV-402, Mitutoyo Instruments, Tokyo, Japan). A 2-µm diamond stylus was used to determine the center line average roughness (R_a) along a length of 10mm. Three individual measurements, between which the distance was 200 µm, were made for each specimen to obtain accurate data regarding the surface roughness.

2. 3. Cell culture

Ultrasonically cleaned samples were sterilized in an autoclave at 120^{o}C for 20 min. MC3T3 mouse osteoblast cell lines were seeded on modified Ti surfaces in 24-well culture plates with a seeding density of 5×10^{4}cells/cm^2 and were incubated at 37^{o}C and 5% CO_2 in humidified air. A α-MEM (Gibco Co., USA) containing 10% fetal bovine serum (FBS, Gibco Co., USA), 500 unit/ml of penicillin and 500 unit/ ml of streptomycin (Gibco Co., USA) was used as the media, which was refreshed every three days. At the prescribed time, the cell culture medium was aspirated from the wells and the substrates were gently rinsed three times with PBS to remove any non-adherent cells. At different time points, the adherent cells were evaluated for their viability using a MTT assay. They were also evaluated for the level of cell attachment and proliferation.

2. 4. MTT assay

A 3-(4, 5-dimethylthiazol-2-yl)-2, 5-diphenyl tetrazolium bromide (MTT) assay was used to evaluate cell viability and cell proliferation. The MTT activity in triplicate samples per group was evaluated. 18 ml of α-MEM without FBS and 2 ml of MTT (Sigma Aldrich) solution were mixed. 1000µl of

the MTT mixture solution was added to the aspirated wells and incubated for 4 hrs at 37°C in a 5% CO_2 atmosphere. The medium was then removed and the dark blue crystals left in the wells were dissolved in 1000μl of dimethyl sulfoxide (DMSO) (Duksan Pure Chemicals Co. Ltd., Korea). The solution was then transferred to a new 96-well micro-plate reader, and the optical density of the solution in each well was measured using a spectrophotometer at a wavelength of 570nm. Analysis of variance (ANOVA) was used to examine the differences in cell viability between the groups.

2. 5. Statistics

The surface roughness and MTT assay results are expressed as the mean ± standard deviation with n = 3. The error bars in the figures represent the standard deviations. Differences between the experimental groups were analyzed using to a paired Student's t-test with $p<0.05$ considered to be statistically significant.

3. Results

Figure 1 shows a morphological assessment of TiO_2 particles obtained by heating and quenching pure Ti at 600°C, 700°C, 800°C, 900°C and 1000°C, respectively. The surfaces showed noticeable changes as the heating temperature increases. The particles are globular with a grainy surface structure. Most of the TiO_2 particles were round with a smooth surface, although the larger TiO_2 particles were typically elongated and rough. From SEM images, crystallites 0.02μm to 0.07μm in size were observed on the surface of the samples heated to 600°C and 700°C. Those of the 700°C group were more densely distributed compared to those of the 600°C group. The particles

became more densely distributed as the heating temperature increased. The crystallite size increased as the temperature of the thermal treatment increased. The average crystallite size ranged from 0.1µm to 0.3µm for the samples heated to 800^{o}C, from 0.3µm to 0.5µm for those heated to 900^{o}C, and from 0.7µm to 0.9µm for those heated to 1000^{o}C.

The surface roughness of the quenched surface at different temperatures was determined using Surftest Formtracer, which gives the average roughness of the surfaces. The average roughness is the roughness parameter that is most commonly used. As shown in Figure 2, statistical analyses indicate the influence of the heating and quenching temperature on the surface roughness of titanium. The surface roughness gradually increases as the heating temperature increases, and a significant difference in the roughness was observed. The average roughness values ranged from 0.15µm to 1.07µm.

Figure 3 shows XRD patterns after heating and quenching pure titanium at different temperatures. Characterizing the crystal structure of naturally oxidized films on titanium metal using ordinary XRD is very difficult because the film thickness is very thin at a few nanometers and has an amorphous structure [138] (not shown in the figure). The rutile structure of titanium oxide, which is more stable than the anatase structure in a thermal atmosphere, was observed in all sample groups; however, the intensity of the peaks differs under different heating temperatures. The main rutile peak was obtained at the (110) plane. The crystallite size was estimated from the full width at half maximum (FWHM) of the (110) diffraction peak using the Scherrer formula.

$D= k\lambda/\beta\cos\theta$

Here, D is the crystallite size (nm), k is the shape coefficient (0.9), λ is wave length (nm), θ is diffraction angle (^{o}), and β is the angular width of the (110) peak at half of its maximum intensity (FWHM). The decreasing the value of FWHM is due to the increase of the crystallite size [165]. The calculated result shows that crystallite size increases as the heating temperature increases.

Figure 4 presents the results of the cell toxicity evaluation conducted by measuring the optical density using the MTT assay after cultivating MC3T3 cells for three days by applying titanium surface heating and quenching at different temperatures of 600^{o}C, 700^{o}C, 800^{o}C, 900^{o}C and 1000^{o}C. The optical density value increased gradually as the heating and quenching temperature increased. The optical density of the titanium surface heated and quenched at 1000^{o}C had higher values relative to those of the other groups.

4. Discussions

Interactions between biomaterials and cells mainly depend on the surface characteristics of the biomaterials, including the surface topography, chemistry and charge. The results of this study show that the surface morphology, crystalline structure, surface roughness and cellular response of oxide film differed as the heating and quenching temperature changed. XRD analysis showed that the surface oxide of the heat-treated and quenched titanium metal at different temperatures was rutile TiO_2. Other oxides of titanium were not detected. From chemical thermodynamics, the formation of rutile TiO_2 is a favorable process, as the Gibbs function of the formation of the rutile type ($\Delta_f G_{m,298K}$ = -888.67 KJ mol^{-1}) is lower than that of the anatase type ($\Delta_f G_{m,298K}$ = -883.65 KJ mol^{-1}) [166]. Other titanium suboxides, such as Ti_2O_3 and TiO,

can also form in some cases [167-170]. However, in this study, sufficient oxygen at a high temperature would convert titanium suboxides, even if they might instantaneously form, to TiO_2 with the highest oxidation state. This occurs because titanium has a strong affinity for oxygen and because TiO_2 is most stable thermodynamically [171].

SEM analysis indicated that the heat treatment and subsequent quenching roughened the surfaces of the titanium plates. That is, heat-treated and quenched titanium sample surfaces had larger total surface areas compared to untreated titanium samples. Clearly, a larger surface area would be more apt to produce more active sites on the surfaces along with active hydroxyl groups. The content of the hydroxyl groups, which have a negative charge, was an important factor in the surface modification of implants, as it positively affects bone growth as well as cellular interactions when titanium is used in dental implants. Numerous parameters are related to the content of the hydroxyl groups.

The surface properties of an implant have a crucial role in cell adhesion and proliferation. The different morphologies and roughness levels for different surfaces lead to different interactions of cell materials. Greater osteoblast adhesions were directly related to increased surface roughness values. After heat oxidation, the surface roughness of rutile films increased in the order of 600°C, 700°C, 800°C, 900°C and 1000°C (Figure 2). From a MTT assay, the roughened surfaces showed more favorable attachment characteristics and differentiation of the osteoblasts, as the filopodia extensions coming out from the cell grasp the granulated patterned rough surface for anchorage. This is in

agreement with published reports. The rougher surface of Ti promoted greater osteoblast-like cell attachment.

The effect of the surface properties on cells by physiochemical interactions generally occurs at the initial stage of cell attachment. The present results show, on the whole, that the surface topography, roughness and chemistry have an influence on cell growth and cell function.

5. Conclusions

The micromorphology, crystallinity, crystallite size and cellular interactions of titanium oxide films were influenced by differences related to a thermal treatment and subsequent quenching. Granular oxide with a rutile structure was observed in the Ti-600 and Ti-700 sample groups. Crystallites of a larger size with a rutile structure were observed in the Ti-800, Ti-900 and Ti-1000 groups. The crystallite sizes of those groups increased as the treatment temperature increased. It was observed that greater surface roughness was obtained as the heating temperature increased. The greater surface roughness, higher surface energy and additional surface hydroxyl groups resulted in greater numbers of attached osteoblasts and higher cell activity. The results of a MTT assay showed that higher cell proliferations were obtained in the Ti-1000 sample group.

Samples	Average roughness R_a (μm)			Mean R_a (μm)	Standard deviation
	Test 1	Test 2	Test 3		
Control	0.141	0.170	0.153	0.154	0.01457
Ti-600	0.193	0.207	0.203	0.201	0.00642
Ti-700	0.243	0.256	0.254	0.251	0.01962
Ti-800	0.355	0.340	0.394	0.363	0.02156
Ti-900	0.705	0.734	0.754	0.731	0.01754
Ti-1000	1.121	1.046	1.061	1.076	0.05111

Table 3. Surface roughness values on different sample groups

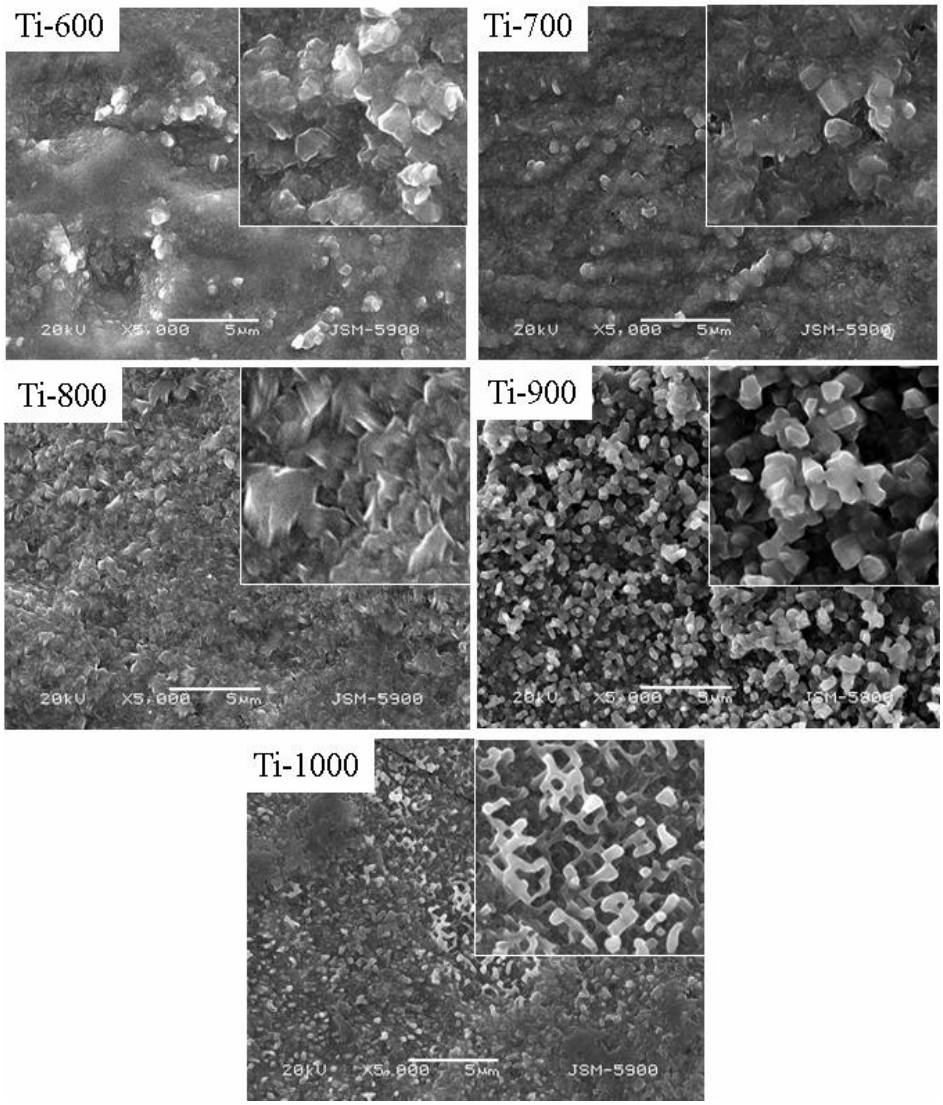

Figure 1: SEM photographs of different sample groups

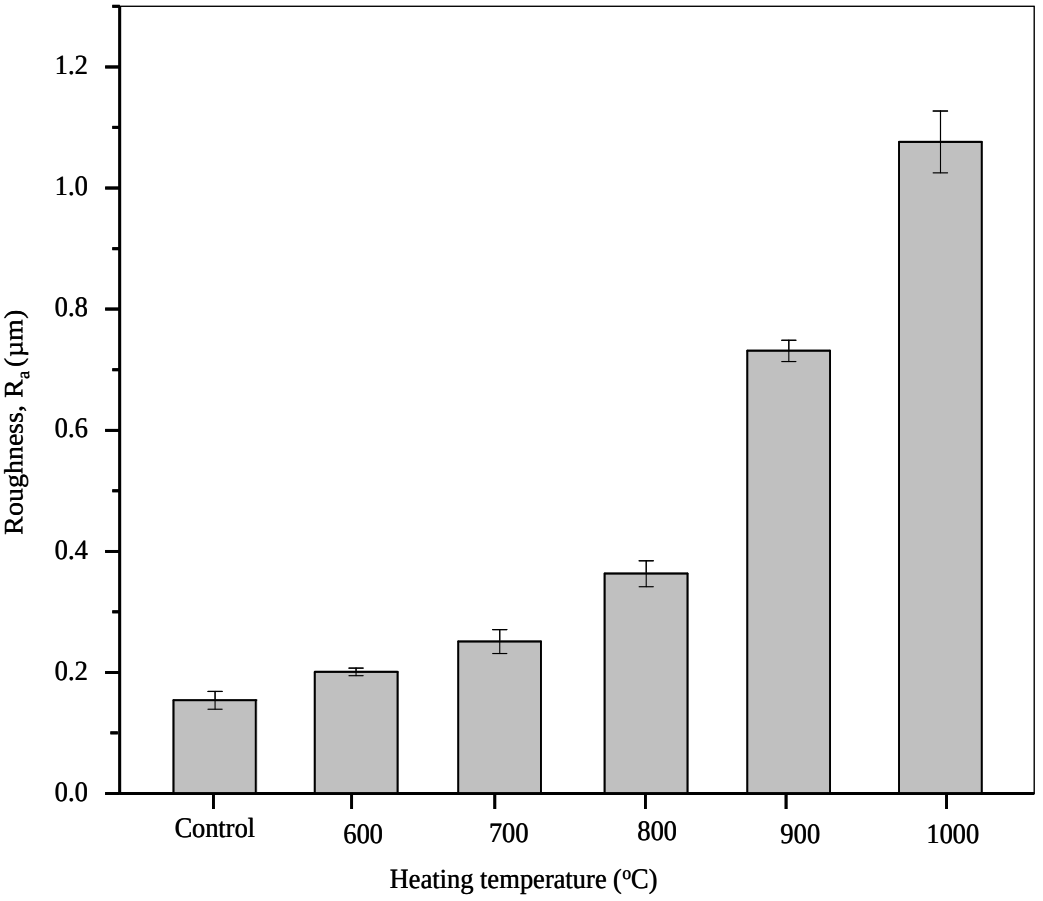

Figure 2: Surface roughness of Ti plates

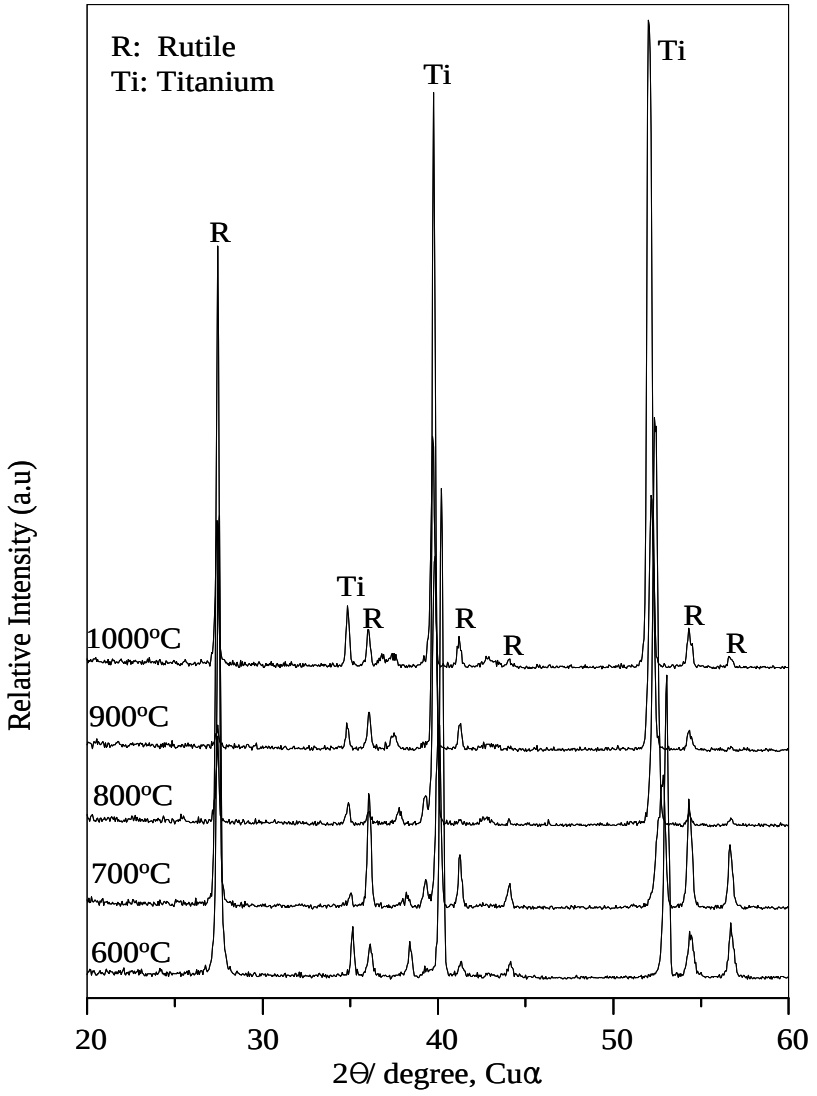

Figure 3: XRD patterns of different sample groups

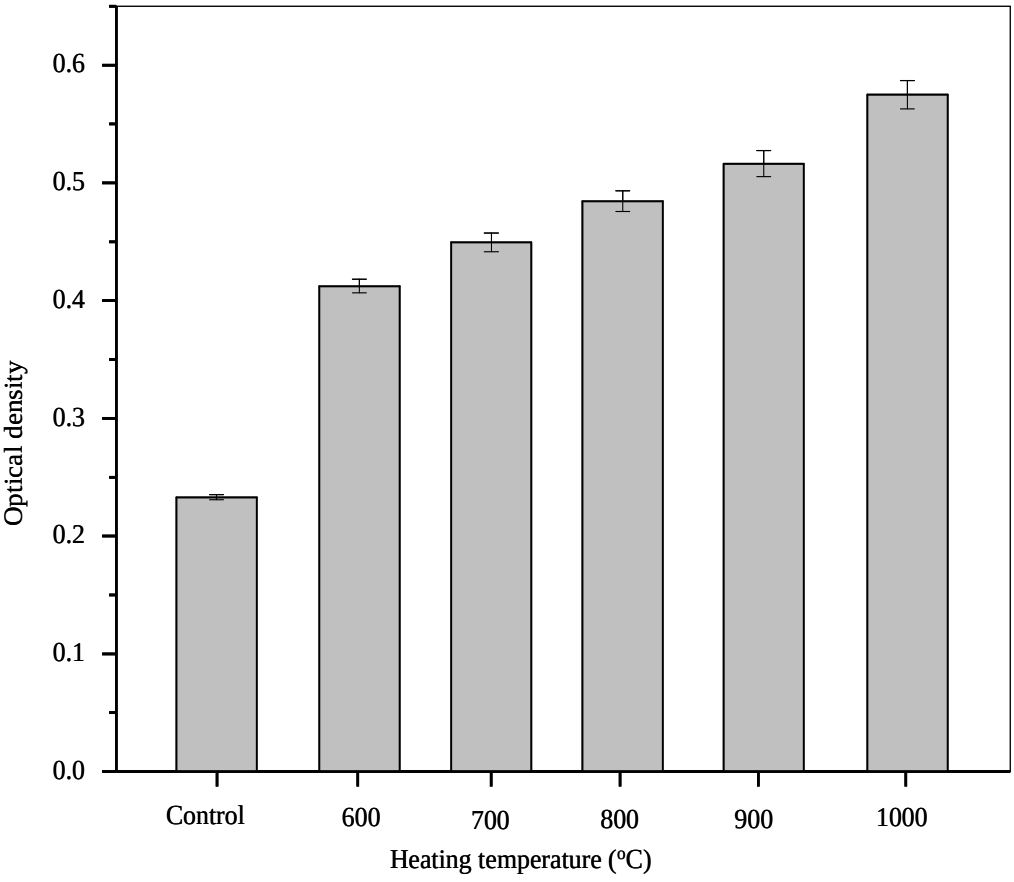

Figure 4: MTT assay data showing the optical density of the reaction product of the MTT working solution with osteoblast cells cultured using different heating and quenching surfaces after 72 hours of incubation.

III. Anodic oxidation of titanium: Influence of pH on the formation of oxide and in vitro osteoblast response

Present study dealt the surface morphology, microstructure, and chemical composition of titanium surfaces treated by anodic spark oxidation in phosphate buffer solution at pH 2, 7 and 12. The pH of the electrolyte was found to play a substantial role in the formation of different morphologies, chemical compositions, and pore dimensions with microporous structures. SEM revealed variation in the topologies of the anodized surface with electrolyte pH. Porous structures with uniform pores and high roughness were obtained in pH 12 solutions. However, intense anatase crystal was obtained at pH 7. The relationship between surface characteristics of titanium and initial interactions of titanium-osteoblasts was also investigated. Our findings demonstrated the cell viability and proliferation on the anodic oxides produced at pH 12 to be superior to those produced at pH 2 and 7 as well as on the control titanium surface. This study also provides evidence of enhanced osteoblast adhesion on anodized metal substrates under in vitro conditions.

1. Introduction

Titanium and titanium alloys have been used as major components in dental and orthopedic implants for many years because of their mechanical strength and relatively high degree of biocompatibility. As suggested by Steinemann [172], titanium is “the material of choice” for hard tissue replacement on account of its high chemical stability in the body, which is the result of the passivating native oxide film of TiO_2 [173]. It also has suitable

physical properties. However, even if titanium osseointegrates, it is only passively integrated in the bone, and, as with other metals, cannot bind directly to the bone. In an attempt to improve the bone bonding ability of titanium implants, many attempts have been made to modify the structure, composition, and chemistry of the titanium surfaces [174–178]. Several techniques for producing a suitable titanium surface to enhance bone growth around implants have been suggested. These include sol–gel deposition [179], ion beam enhanced deposition [180], sputter coatings [181], acid etching [182], and vacuum plasma spraying [183]. In recent years, some coatings have had excellent applications as orthopedic and dental implant materials. However, these coatings often dissolve from the implants, resulting in failure [184] or poor adhesion to the substrate [185]. Therefore, alternative ways for producing porous titania films with strong adhesion to a substrate are under investigation. A potential process for producing oxide films on metals such as aluminum, titanium, magnesium and zirconium was recently reported [186]. The process is called micro-arc oxidation (MAO), and can form ceramic-like films on such metal surfaces with a complex geometry. MAO can produce a porous, relatively rough and firmly adherent oxide layer on a titanium surface [187, 188]. The porous nature of the anodized films increases the anchorage of implants to the bone and opens up the possibility of the incorporation and release of antibiotics around the titanium implants [189]. This process combines electrochemical oxidation with a high voltage spark treatment in an aqueous electrolyte containing modifying elements in the form of dissolved salts such as Ca and P ions or Ca ions or P ions. In the case of MAO, the

growth behavior of the oxide film on cp titanium metal is strongly dependent on the electrolyte used and on the anodization parameters such as the electrolyte concentration, the electrolyte temperature, applied voltage, and current density [190, 191]. H_3PO_4 and H_2SO_4 at different concentrations [192], and $(NH_4)_2SO_4$ or $NaHCO_3$ solution containing fluoride ions are the most commonly used electrolytes in titanium anodization. The effect of the electrolyte composition and current density on the characteristics of MAO films on titanium alloys has been reported [193-196]. Schmuki and co-workers [197-199] examined the effect of the solution pH on the size and shape of the TiO_2 nanotubes formed by anodization. Further improvement in coating growth and microstructure can be achieved by adjusting the electrical parameters or the selection of electric control modes.

This study examined the effect of the electrolyte pH for titanium oxidation in a phosphate buffer electrolyte on the phase of TiO_2 in the oxide layer. In particular, the relationship between anatase formation and the electrolyte pH was examined. The electrolyte pH also influences the surface roughness, microstructures, and pore dimensions of microporous surface. In addition, a biological evaluation of the anodic TiO_2 films formed in electrolytes at different pH was carried out in seeding osteoblast cells on anodized titanium surfaces. The pH selection of the electrolyte was based on the pK_a values of the phosphoric acid used in the buffer because a buffer with a pH = $pK_a \pm 1$ is biologically important and more effective.

2. Materials and methods

2. 1. Anodic oxidation of titanium

2. 1. 1. Substrates

Specimens of commercially pure titanium plate grade two (20mm × 10mm × 2mm) were abraded with 220 to 800 grits SiC paper to remove surface impurities. The specimens were chemically pickled with a solution containing 55 mass % HF, 65-68 mass % HNO_3 and distilled water at a ratio of 1:3:6 in a volume for passivation; specimens were then ultrasonically cleaned in double distilled water, and dried.

2. 1. 2. Surface modification

The anodization system included a power supply, an electrochemical cell, a platinum sheet cathode, accessories to connect the electrodes to the power supply, and a magnetic stirring apparatus, in which the substrates of interest were used as the anode (Figure 5). The anodization process was carried out in an electrochemical cell containing 0.1M phosphate buffer solution at room temperature under continuous magnetic stirring. The electrolyte was prepared using phosphoric acid and its potassium salts (KH_2PO_4 and K_2HPO_4 Sigma Aldrich) at pH 2, 7 and 12. The pH of the electrolyte was adjusted using either 1M KOH or 1M H_3PO_4. Oxidation was carried out in a two-electrode setup with a titanium plate anode and a platinum plate cathode. Well-defined porous morphologies were obtained using an anodizing potential of 350 V at an anodic current density of 30mA/cm^2 with sparks on the titanium surface. The anodized samples were cleaned ultrasonically with double distilled water and dried at room temperature.

2. 1. 3. Characterization of anodic films

The surface composition and morphology of the titanium surface after anodic oxidation was examined by scanning electron microscope (SEM) (JEOL JSM-5900, Japan) connected to an energy dispersive X-ray spectrometer (EDS). The crystalline structure was identified via X-ray diffraction (XRD) (Dmax III-A type, Rigaku Co., Japan) using Cu Kα incident radiation, a tube voltage of 40 kV, a current of 30 mA, and, from 20^o to 60^o 2θ, a scanning rate of 4^o/min. The surface roughness of the material was measured using a Surftest Formtracer (Surftest SV-402, Mitutoyo Instruments, Tokyo, Japan).

2. 1. 4. Cell culture

MC3T3 mouse osteoblast cell lines were isolated from bone samples. The cells were seeded on the titanium plates at 5×10^4 cells/cm^2. All samples were incubated in Minimum Essential Medium (α-MEM, Gibco Co., USA) with 10% fetal bovine serum (FBS, Gibco Co., USA), 500 unit/ml of penicillin, and 500 unit/ml of streptomycin (Gibco Co., USA) at 37^oC in 5% CO_2 atmosphere. After incubation for the prescribed time, the samples were removed and assayed for MTT.

2. 1. 5. MTT assay

A 3-(4, 5-dimethylthiazol-2-yl)-2, 5-diphenyl tetrazolium bromide (MTT) assay was used to evaluate cell viability and cell proliferation. 18 ml of α-MEM without FBS and 2 ml of MTT solution were mixed. 10^3 µl of the MTT mixture solution was added to the aspirated wells and incubated for 4 hrs at 37^oC in a 5% CO_2 atmosphere. The medium was then removed and the dark blue crystals left in the wells were dissolved in 10^3 µl of dimethyl sulfoxide (DMSO)

(Duksan Pure Chemicals Co. Ltd., Korea). The solution was then transferred to a new 96-well micro-plate reader, and the optical density of the solution in each well was measured using a spectrophotometer at a wavelength of 570nm. Statistics in cell viability were performed by analysis of variance (ANOVA), followed by a Student's t-test to determine the significance of differences between the groups.

3. Results and discussion

3. 1. Structures of titanium metal surfaces after anodic oxidation

It is known that the properties of surface oxide are responsible for biologic response to titanium implants. In the present study, anodic oxidation at different electrolyte pH produces different topographies and chemical compositions of surface oxides on titanium. The morphology, roughness, and structure of anodic oxide film of titanium depend primarily on preparation procedures, anodizing variables, and types of electrolytes [195, 200]. Considering all anodizing variables at the same time makes the research very complex; hence, we chose one very different anodizing variable: "electrolyte pH". There are very few research works on anodization of titanium that study the effect of electrolyte pH. The following discussion will be focused on the morphology and phase composition of oxide films obtained at 350 V potential and 30mA/cm^2 current density at different electrolyte pH.

When titanium metal was anodically oxidized in 0.1M phosphate buffer solutions of pH 2, 7 and 12, the surfaces become porous at the DC voltage with a spark discharge occurring and the anodic oxide film was observed to contain P, suggesting that the P-containing anodic oxide film enhances the absorption

of P and uptake of calcium from the biologic environment to form calcium phosphate [201]. This method is a desirable means of improving the pace of surface activation and osteosynthesis when an implant is set in bone by absorbing Ca and P or Ca or P from the electrolyte solution to the porous oxidation surface layer. Ishizawa et al. [202] reported that thin and rough porous TiO_2 layers that absorb Ca and P from an electrolyte solution containing Ca and P can produce a bioactive oxide film with acceptable cell compatibility. Regarding this surface treatment, the porous layers absorb P from electrolyte. The content of phosphorous on the oxide surface differs as the electrolyte pH variable.

Figure 6 shows the porous surface morphology of the anodic oxide films that were treated at different electrolyte pH; the pores are well separated and homogeneously distributed over the surface. The anodic oxide films in aqueous phosphate buffer were observed to have overlapping micro-domains consisting of pores at pH 2 anodized surfaces. The size of micro-domains on the oxide film decreased with an increase in the electrolyte pH. The morphology of the anodized titanium changes with electrolyte pH containing P ions, forming porous oxide films. The density of pores formed above breakdown potential increases with electrolyte pH. The size of the pores, which originate from sparks on the interface of oxide and electrolyte, was related to the nature and pH of electrolyte. Closer examination of coatings revealed details of the pore morphologies. The coating formed at pH 12 was of relatively uniform morphology, with pores of size ~ 1.0 to1.7 μm in diameter (Figure 6(c)). At pH 7, pores of increased size ~1.8 to 2.5 μm were observed (Figure 6(b)). At pH 2,

the pores were of size ~1.0 μm, some larger pores were observed due to interconnection of adjacent pores (Figure 6(a)). Further, relatively fine pores could also be seen in the coating material inside the larger pores at pH 2 and 7 anodized surfaces (Figure 6(a) and (b)). However, the surface oxide is covered with a compact thin oxide film due to the intrinsic property of the metal [203]. Thus, anodic oxidation at pH 12 became active and vigorous, resulting in the formation of similar-shaped pores/craters distributed homogenously over the surface. This variation in morphology, pore distribution, and dimensions are due to the pH change in electrolyte. As the pH changes, the ionization of the electrolyte alters and has different interaction with metal surface. Results of the EDS analysis of the anodic oxide films are shown in Figure 6 below SEM image. As the electrolyte pH decreased, an increase in P concentration and a decrease in Ti concentration were observed. Similarly, as the electrolyte pH decreased, the O/Ti ratio increased. This suggested that the negatively charged P ions migrated into the oxide under the electric field during anodization and thus resulted in a more rapid oxide growth. Leach and Pearson [204] reported that the level of incorporation of foreign anions was higher in acid solutions, which are enhanced by the presence of space charge defects in the oxide. Therefore, the number of P ions integrated on the oxidation layer is inversely proportional to the electrolyte pH. The incorporation of negative phosphorous ions into the oxide film provides the compositional basis for the formation of calcium phosphates, primary inorganic phases of hard tissues, and has the osteoinductive properties in physiological fluids. This is because during MAO process phosphorous anions electrochemically incorporated into the TiO_2

matrix to form phosphated titanium oxide. Phosphated titanium oxide, when it comes in contact with physiological fluids, enhances the rapid growth of bone tissue. EDS revealed the presence of P, Ti and O in the oxidation layer, which indicates that the P ions in the electrolyte are involved in the physicochemical reaction associated with the MAO process.

Figure 7 shows the X-ray diffraction patterns of the anodic titania film formed at different electrolyte pH. The anodic oxide consists of a mixture of amorphous and anatase oxides. As the electrolyte pH varied, the degree of oxide crystallinity also changed. Using the peak heights of the titanium substrate as references, the thickness of the oxide film was observed to change as the electrolyte pH varied. From the baseline of the spectra, it was seen that change in electrolyte pH resulted in change in the amorphous oxide. The anodic oxide film was its most crystalline form at pH 7 in 0.1M phosphate buffer solution. This is because the oxide that grows in near neutral solutions is not very soluble. However, at pH 2 the intensity of oxide film decreased because the deposition and dissolution of porous oxides take place in acidic electrolytes at the same time. Similarly, at pH 12 after the formation of oxide passivations occurred on the titanium surface, no more oxide films were formed. Also, passivation treatments provide a controlled and uniformly oxidized surface state. Passivation leads to stable oxide film and improves corrosion resistance [205]. The enhancement of corrosion resistance, in turn, suggests an increase in biocompatibility of titanium [206]. The crystallinity of the TiO_2 layer was found to increase with increasing oxide thickness [175, 207]. This suggests that the most porous and most crystalline TiO_2 can be produced near physiological

pH. However, differences in oxide crystallinity were not observed to affect initial osteoblast precursor cell attachment.

The presence of porous surfaces on the anodic oxide was suggested to increase the surface roughness and energy, and might cause microscopic tissue-cell ingrowth, which would improve implant fixation [208]. It is generally accepted that high roughness and porous structure led to better cell attachment. Keller et al. [209] claimed that in vitro cell attachment of MC3T3 osteoblast is directly related to the surface roughness of titanium. Table 4 shows the average roughness values for different surfaces. There is almost an order of magnitude difference in roughness for the Ti-control and anodized surfaces. The roughness of anodized surface was higher than the original surface before it was anodized. Three disks were measured from each of the three different surfaces to obtain an average roughness value R_a. There were statistically significant differences in R_a between the four groups. As electrolyte pH changed, change in the roughness of anodic oxide films was observed. The lowest roughness was observed in the control group and the highest was observed in the plate anodized in the pH 12 solution. The R_a values of the prepared titanium disk ranged from 0.2 μm to 0.5 μm. This suggests that the average surface roughness is a function of the electrolyte pH. As a result, anodic oxidation of the titanium implants demonstrated changes in the various oxide properties such as the oxide thickness, surface morphology, pore diameter, crystallinity, chemical composition and surface roughness [210].

3. 2. MTT assay

Figure 8 shows the result of cell viability measured using the MTT assay. The amount of the formazan product generated from the process (in Materials and Methods) is proportional to the number of live cells, even though the absolute absorbance for a given cell number varies between cell lines. The metabolism of MTT was poor on the untreated and anodized titanium surface at pH 2 and 7 with low absorbance values. But MTT metabolism was quite good on anodized surface at pH 12, with superior absorbance value. This suggests that due to the more porous and rougher surface, more cells were attached on the surface. This indicated that the electrolyte pH influenced cell viability on the anodized titanium surface, although no statistical difference was observed among these groups. However, similar seeding cell numbers were used in each assay because culture conditions such as the cell density can significantly affect the results of the MTT assays. This suggests that a surface anodized at pH 12 may be a suitable material for biomedical applications in comparison to other surfaces.

3. 3. Mechanism of TiO_2 deposition and growth model

The anodic oxidation of a metal occurs as a result of erosion from the metal surface and deposition from the electrolyte. The erosion and deposition process occurs simultaneously so that the metal surface forms a homogenous oxide layer. The surfaces of anodized valve metals, particularly aluminum, have two layers, inner and outer [211]. The inner layer exposed to the electrolyte contains anions from the solution; the outer layer is considered to be

free of anions and is essentially a barrier layer-type material. A similar oxide structure can also be expected in the case of anodized titanium.

The general reactions that take place during anodic oxidation of titanium are as follows.

At Ti/Ti oxide interface:

$Ti \rightarrow Ti^{2+} + 2e^{-}$ (1)

At Ti oxide/electrolyte interfaces:

$2H_2O \rightarrow 2O^{2-} + 4H^{+}$ (oxide ions react with Ti to form oxide) (2)

$2H_2O \rightarrow O_2$ (gas) $+ 4H^{+} + 4e^{-}$ (oxygen gas evolves or sticks to the electrode surface) (3)

Both interfaces:

$Ti^{2+} + 2O^{2-} \rightarrow TiO_2 + 2e^{-}$ (4)

Reactions (1) (2) and (3) are believed to occur at the metal/oxide interface and oxide/solution interface to form oxide layer on the titanium surface, respectively. These three reactions are for the formation of a barrier type layer. Reaction (4) indicates the formation of an oxide in the presence of oxide ions and dissolved titanium cations in the electrolyte solution. TiO_2 can precipitate and form inner wall layers in the porous structure.

From the above observed facts, the formation of porous titanium may be described as follows. As the voltage increases, a thin non porous titania layer grows on the titanium surface (Figure 9 (a)). Then, due to the volume changes accompanying the oxidation of titanium, stresses exist in the oxide layer that supports the formation of crystalline oxide [209]. When oxide layer changes to a dense crystalline form, the stress in the oxide obviously decreases. This

crystallographic transformation is closely related to the breakdown [209]. Selective dissolution takes place due to different stresses and crystalline state; then, small pits originate in the oxide layer as in (Figure 9 (b)). As the oxidation increases, breakdown of the barrier oxide film occurs and new deep pores between crystallites are formed (Figure 9 (c)). This corresponds to the occurrence of sparking and the areas of electrical breakdown of the oxide immediately undergo repassivation (Figure 9 (d)) due to the characteristics of valve metals. When the breakdown occurs again inside the repassivated pores (Figure 9 (e) and (f)), it looks as though there is the formation of small pores inside the pores. Since current can flow through the whole oxide layer, the thickness of oxide cannot linearly increase with anodizing time.

4. Conclusions

Anodic oxide film of titanium produced using phosphate buffer solution was observed to consist of a porous or non-uniform layer and a dense or uniform layer. A more porous surface with superior surface roughness was obtained at pH 12 anodized surfaces. XRD and EDS analysis indicated that the film consists of a mixture of anatase and amorphous oxide, with the incorporation of phosphorous. The degree of oxide crystallinity was observed to vary with electrolyte pH. In addition, the concentration of P ions increased as the electrolyte pH decreased. MTT assay shows no significant difference in the cells cultured on all surfaces but the pH 12 anodized surfaces showed a slightly superior result. As such, it was concluded that the electrolyte pH plays an important role in governing oxide thickness, composition, degree of oxide crystallinity, and also the biocompatibility of anodized surface. Further in vivo

studies with animal models are necessary for a better comparison of the osseointegrative properties of these different surfaces.

Roughness of anodic oxide films of titanium

Specimens	pH of electrolyte	Current density (mA/cm^2)	Final voltage (V)	Roughness ± SD		
				R_a (μm)	R_y (μm)	R_z (μm)
Control Ti	—	—	—	0.212 ± 0. 008	1.782 ± 0. 258	1.144 ± 0. 043
1	2	30	350	0.353 ± 0. 021	3.071 ± 0. 202	2.232 ± 0. 091
2	7	30	350	0.485 ± 0. 025	4.287 ± 0. 284	3.180 ± 0. 209
3	12	30	350	0.544 ± 0. 065	4.423 ± 0. 674	3.056 ± 0. 322

n = 3, SD = Standard Deviation

Table 4. Roughness of the control and anodized titanium plate

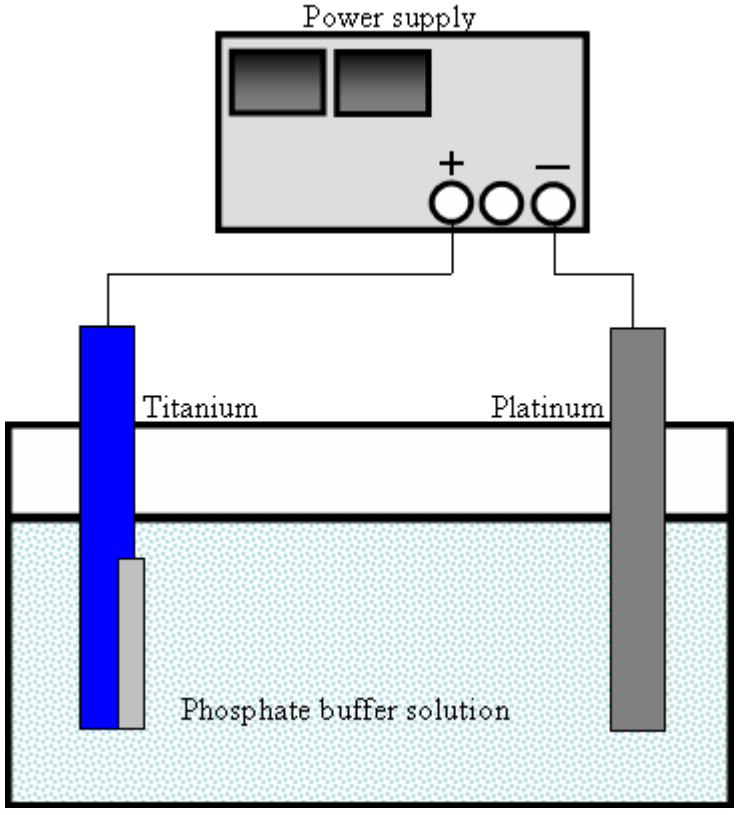

Figure 5. Schematic diagram of anodization

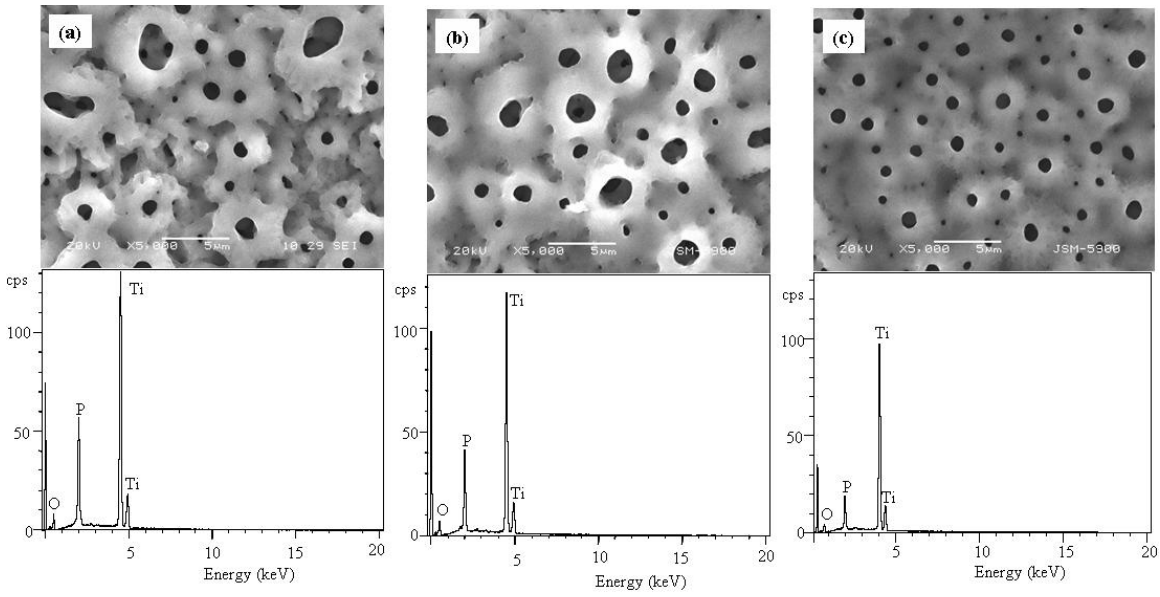

Figure 6. SEM micrographs with the EDS spectra of the titanium metals anodically oxidized at 350 V, 30 mA/cm^2 in phosphate buffer solution (a) pH 2 (b) pH 7 and (c) pH 12

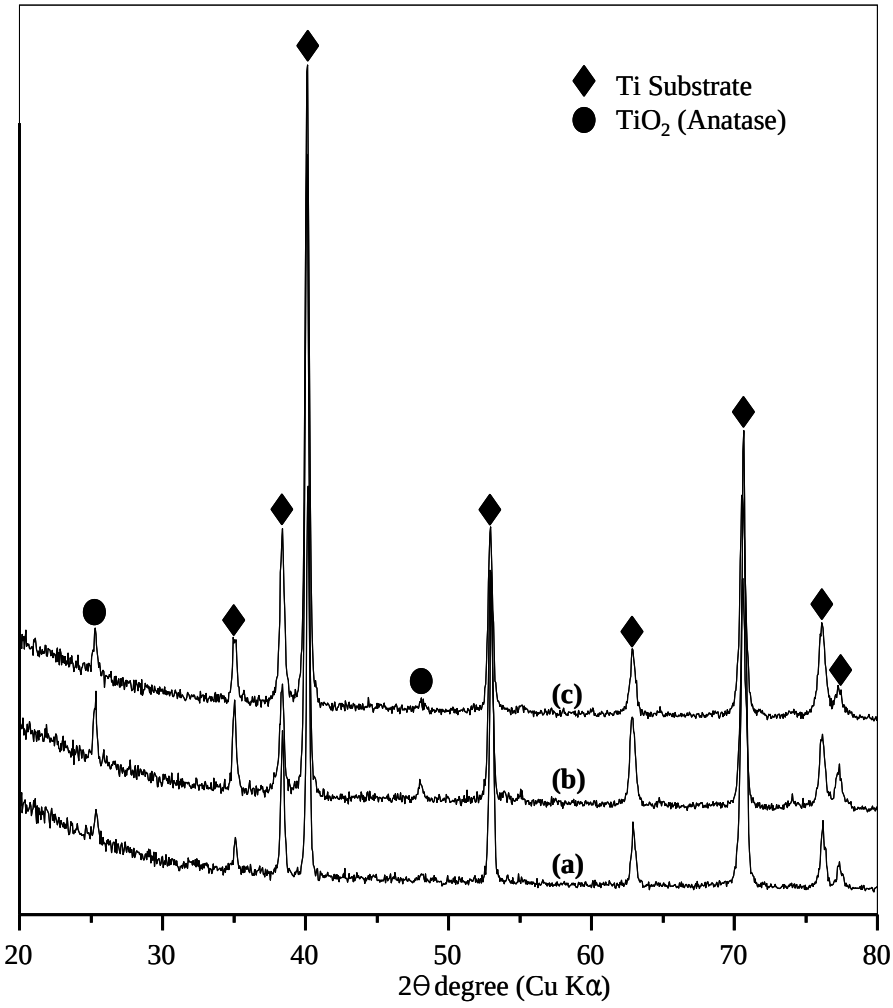

Figure 7. XRD patterns of the anodic oxide films on the titanium surface at 350 V and 30mA/cm^2 in phosphate buffer solution: (a) pH 2 (b) pH 7 (c) pH 12

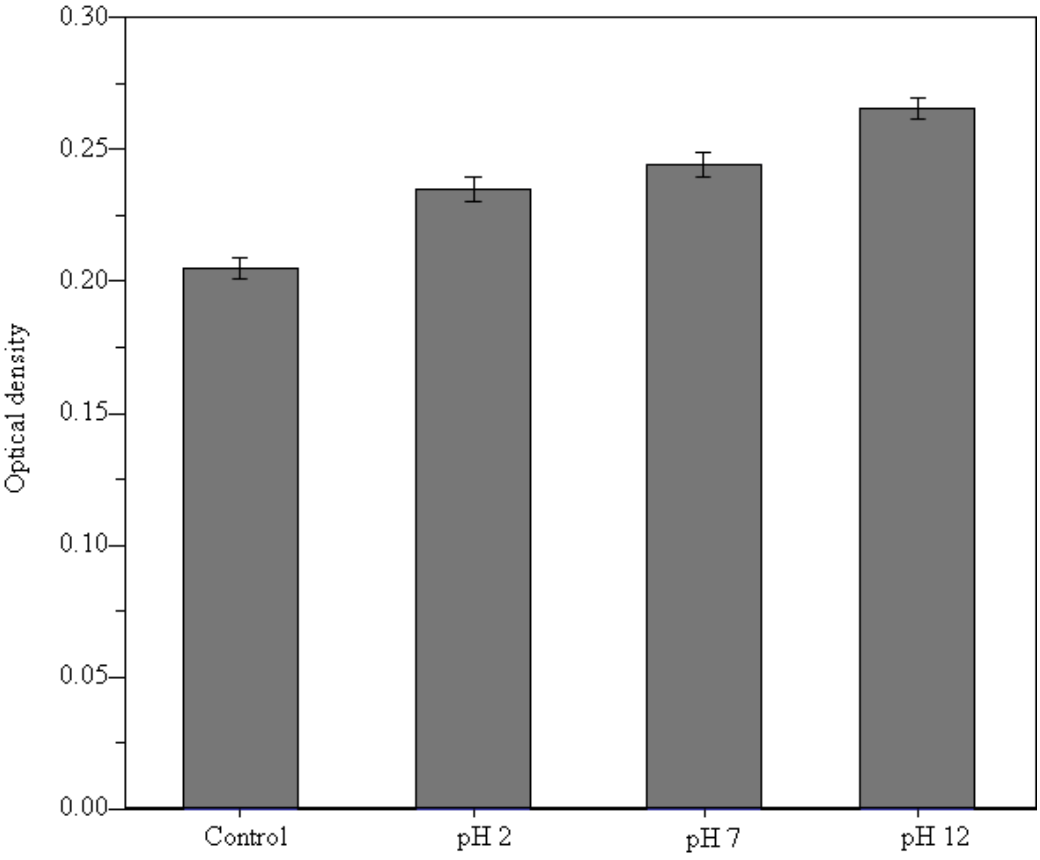

Figure 8. Optical density measured after culture for 3 days at a wavelength of 570nm using an ELISA reader (n=3 per group)

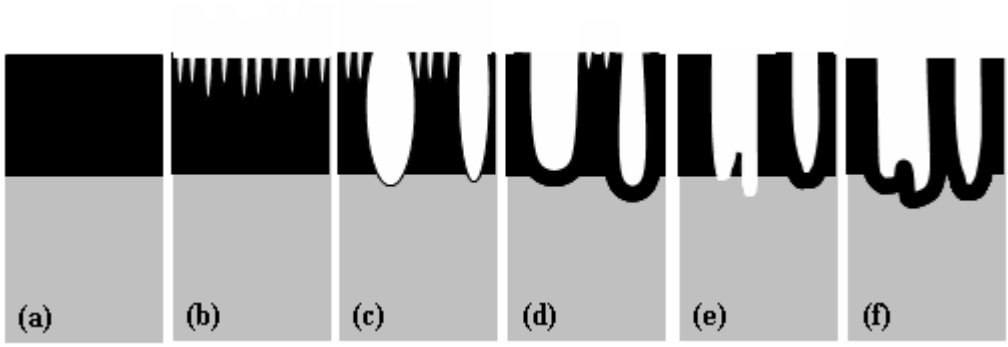

Figure 9. Schematic diagram of porous titanium oxide formation above the breakdown potential: (a) Oxide layer formation on metal surface (b) burst of oxide by the formation of crystallites (pore formation) (c) Growth of pores due to field assisted dissolution of titania (d) Repassivation of pore tips (e) Burst of repassivated oxide (f) Formation of new pores inside existing pores.

IV. Fabrication of titanium oxide nanotubes by electrochemical anodization in acidic fluoride solution: Study the phase transformation and stability

TiO_2 nanotube array (TN) on titanium plate was fabricated by using an electrochemical method. The crystal structure and surface morphology of TN array was examined by X-ray diffraction (XRD) and Field Emission Scanning Electronic Microscopy (FE-SEM), respectively. The stability of the nanotube structure and crystal phase transition was studied at different temperatures in dry oxygen ambient. The as-deposited films were found to be amorphous. The tubes crystallized in the anatase phase at a temperature of 450^{o}C. Anatase crystallites formed inside the tubes walls was transformed completely to rutile at 500^{o}C in dry environment. With the heating temperature increased the intensity of rutile peak increased with decrease in reflection from titanium. Intense rutile peak was observed at 600^{o}C. The average pore diameter as calculated from FE-SEM images was 50-100 nm. At higher temperature tubular structure completely collapsed leaving dense rutile crystallites. A model was proposed to explain the formation mechanism of TN fabricated on titanium plate in HF/H_2SO_4 electrolyte.

1. Introduction

Nanotubular materials have attracted tremendous attention due to their exceptional electronic and mechanical properties. Since the discovery of carbon nanotubes [212] the extensive research has been carried out to explore nanotubular materials other than carbon, including the oxide materials i.e. titania, alumina, zirconia, and silica. Recent interest has focused on the creation of nanotube structures of these ceramics [213, 214], especially that of titania which has a wide range of technologically relevant applications such as gas sensors, photovoltaics, photo and thermal catalysis, photoelectrochromic devices, and immobilization of biomolecules.

Titania nanotubes of different geometrical shapes and microstructures have been fabricated by many different techniques like sol-gel synthesis, anodization, electrodeposition, sonochemical deposition, and methods involving the chemical treatment of fine titania particles [215, 216]. Many of these fabrication processes are complicated due to the chemical processes involved, on the other hand, we have used a simple anodization technique because this approach is able to build a porous titanium oxide film of controllable pore size, good uniformity and conformability over large area at low cost. However, before using the titania nanotubes prepared by different methods for different applications factors, the crystalline nature of the structure and stability of the desired crystalline phase as well as the stability of the structure itself must be examined.

Processing techniques and parameters influence the crystalline or amorphous nature of the titania nanotubes. The application and properties of Titania depend on the crystallinity and the isomorph. Anatase is preferred catalysis and dye sensitized solar cells [217, 218] where as rutile in dielectrics and oxygen gas sensor [219, 220]. Crystallization or phase transformations take place through nucleation and growth processes. Although crystallization and phase transformations are essential for many applications involving titania, they have adverse effects on the stability of nanoarchitectures, especially when they occur at elevated temperatures. At elevated temperatures, large surface area makes them prone to solid-state sintering, which leads to grain growth, densification, and eventually complete collapse of the structure [221]. In the case of titania, the most common phase transformation is anatase to rutile where rutile is the stable phase of titania.

This paper investigates the oxidation process of titanium in HF/H_2SO_4 solution via constant-voltage experiments. We have subjected titania nanotube arrays prepared by anodization to high-temperature annealing, up to 600^oC in oxygen to understand their temperature stability as well as structural and morphological transformations. A possible growth mechanism is presented.

2. Material and methods

Commercially pure titanium (grade 2) plates (20mm × 10mm × 2mm) were abraded with 220 to 1000 grits SiC paper. Prior to electrochemical treatment the plates were sonicated in acetone, isopropanol, and methanol successively, followed by rinsing with deionized water and dried. The samples were anodized in 1M H_2SO_4/0.16M HF by using a two electrode configuration

with platinum as cathode and titanium as anode. Figure 10 shows schematic diagram of anodization in which voltage is supplied from DC power supply. The TiO_2 nanotubes were prepared using a 20 V anodization voltage and 2 h of anodization time at room temperature with magnetic agitation. During anodization the color of titanium plate normally changed from purple to blue, light green and then finally light red. For a morphological characterization of the samples, a field-emission scanning electron microscope Hitachi FE-SEM S-4800 was used. Structural characterization was carried out by means of X-ray Diffraction (XRD) (Dmax III-A type, Rigaku Co., Japan) using Cu Kα incident radiation, a tube voltage of 40 kV and a current of 30 mA, and from 20^o to 60^o 2θ with a scanning rate 4^o/min. In order to study the crystal phase transition, the nanotube samples were annealed at different temperatures in dry oxygen for 3 h with heating and cooling rates of 10^oC/min.

3. Results and discussion

It was observed that when titanium plates were anodized in HF containing electrolyte and annealed at different temperatures, the surface properties of anodized titanium changed remarkably with heating temperature. Figure 11 shows FE-SEM images of the nanotube arrays prepared using an anodization potential of 20 V and annealed at different temperatures under oxygen. Image of the sample before heat treatment shows morphological variation with annealed sample. As prepared samples shows impurities with unclear nanotubes (Figure not included) while annealing remove surface impurities and obtain clear nanotubes. Also, heat treatment was introduced for complete removal of fluoride to yield pure nanotube [222]. It can be seen that the

nanotube array is uniform over the substrate annealed at 450^{o}C (Figure 11(a)). The average diameter of nanotube as calculated from FE-SEM images was 50-100 nm (Figure 11 (b)). It is difficult to determine the nanotubes length as that requires cleavage of the nanotube sample. The evolution of surface morphology as a result of high temperature annealing in oxygen is also shown in Figure 11. The nanotube architecture annealed at 500^{o}C is shown in Figure 11 (c) and (d). Although the walls of the tubes coalesced, the sample still possesses porosity. The tubes coalesced and formed a wormlike pattern. Images of another sample heated to 600^{o}C are shown in Figure 11 (e) and (f). These images show that the porous structure completely disappeared because of grain growth leaving dense rutile crystallites.

Figure 12 shows the XRD patterns of the 20 V sample annealed at different temperatures in dry oxygen ambient. The as-deposited titania films were found to be amorphous (Figure 12 (a)). Several studies show that the tubes can be converted to anatase at temperatures higher than approximately 280^{o}C in air [223–228] or a mixture of anatase and rutile at temperatures higher than approximately 450^{o}C [223, 224]. Most recently, there are indications that already in the as-formed tubes under certain conditions nano-crystallites can be present [227, 228]. In the diffraction patterns, the anatase phase was appeared at 450^{o}C (Figure12 (b)) and a temperature close to 450^{o}C. At 500^{o}C complete transformation of anatase to rutile occurred (Figure 12 (c)). At 600^{o}C the rutile peak becomes more intense (Figure 12 (d)). It can also be seen from Figure 12 that the reflections from the titanium substrate decreased as the annealed temperature increased and crystallinity of rutile titania increased. This shows

that the titanium substrate became oxidized and transformed to crystalline titania at high temperatures. It indicates that the grain size of rutile progressively increased with temperature after its nucleation. In contrast, the anatase peak gradually disappears. This indicates that the large anatase grains transformed into rutile with the smaller grains remaining anatase.

3. 1. Mechanism for nanotube formation

The anodization of titanium is accompanied with chemical dissolution of titanium oxide. Nanoporous structure is formed by two processes.

(1) Electrochemical etching (2) Chemical dissolution

The competition between electrochemical etching and chemical dissolution determines the structural morphology of nanotubular layer.

Electrochemical etching

Initial oxide layer forms at the surface of titanium as a result of the following anodic reactions.

$Ti + 2H_2O \rightarrow TiO_2 + 4H^+ + 4e^-$

Chemical dissolution

Hydrogen fluoride (HF) is predominant in acidic fluoride solution. In the presence of acidic fluoride solution, the oxide layer dissolves locally [229-231] and a nanotube is created from small pits that are formed in the oxide layer. These pits are created from the following reactions between TiO_2 and HF as shown in the schematic Figure (13).

$TiO_2 + 6HF \rightarrow [TiF_6]^{2-} + 2H_2O + 2H^+$

On the basis of above reaction, a mechanism of titania nanotube formation shown in Figure (13). Initially, a thin layer of oxide forms on the titanium

surface (Figure 13 (a)) which corresponds to significantly drop of current at the first stage of oxidation. Due to volume change in oxidation of titanium, stresses exist in the oxide layer that encourages the formation of crystalline oxide. The stress in the oxide decreases due to transformation of oxide into crystalline form. This transformation is related to breakdown. Then due to difference in stresses and crystalline form, dissolution of oxide takes place to form pits (Figure 13 (b)). The thickness of the oxide film is thicker at the wall of the pore than at the bottom. Thus, the enhanced electrical field intensity at the pore bottom leads to a deepening of pores. The wall of the pit also dissolves in slow rate leads to widening of pores. At the same time the integration by small pores results in the appearance of larger pores. The pits with barrier layer at the bottom called pores and interpores voids start forming (Figure 13 (c)). Thereafter both voids and tubes grow in equilibrium to yield perfect nanotube arrays (Figure 13 (d)).

4. Conclusions

Well-aligned titanium oxide nanotube arrays prepared by anodization of titanium plate were subjected to heat treatments at different temperatures in oxygen. The samples prepared using an anodization voltage of 20 V, consisting of well-defined nanotube arrays were found at 450^{o}C. However, at higher temperatures the crystallization of the titanium support disturbed the nanotube architecture causing it to collapse and densify. When subjected to annealing in oxygen at 500^{o}C, the tubes coalesced completely and formed a wormlike pattern. At 600^{o}C the dense rutile crystals were obtained. The anatase phase was appeared at 450^{o}C through XRD studies. The anatase was completely

converted into rutile at 500^{o}C. Annealing in oxygen to 600^{o}C created a notable change in crystallinity of rutile with decreasing the reflections from titanium.

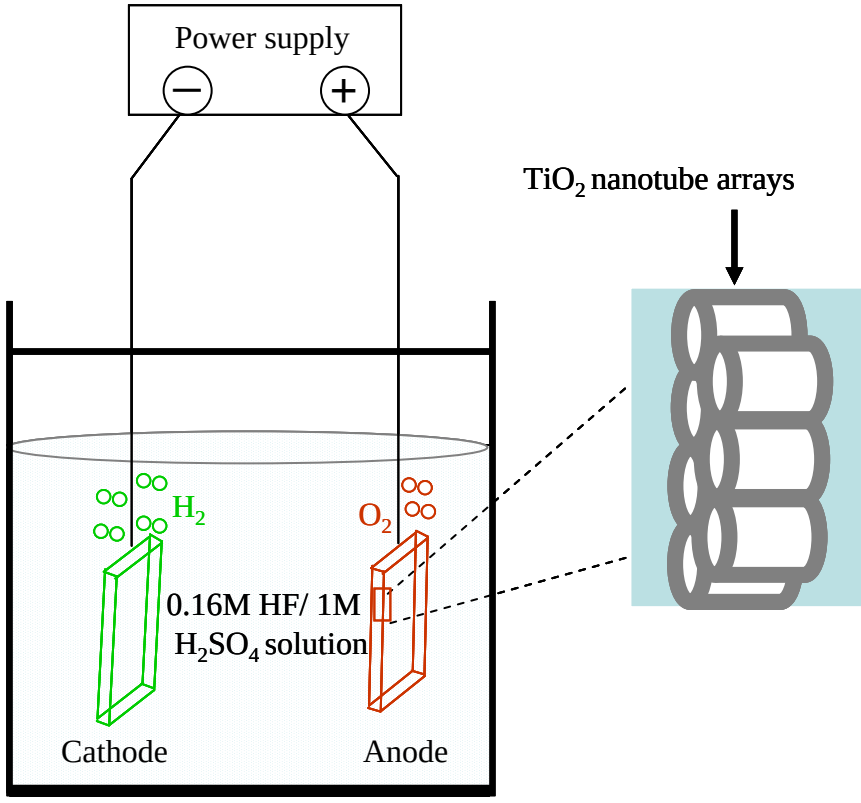

Figure 10. Schematic diagram of anodic oxidation

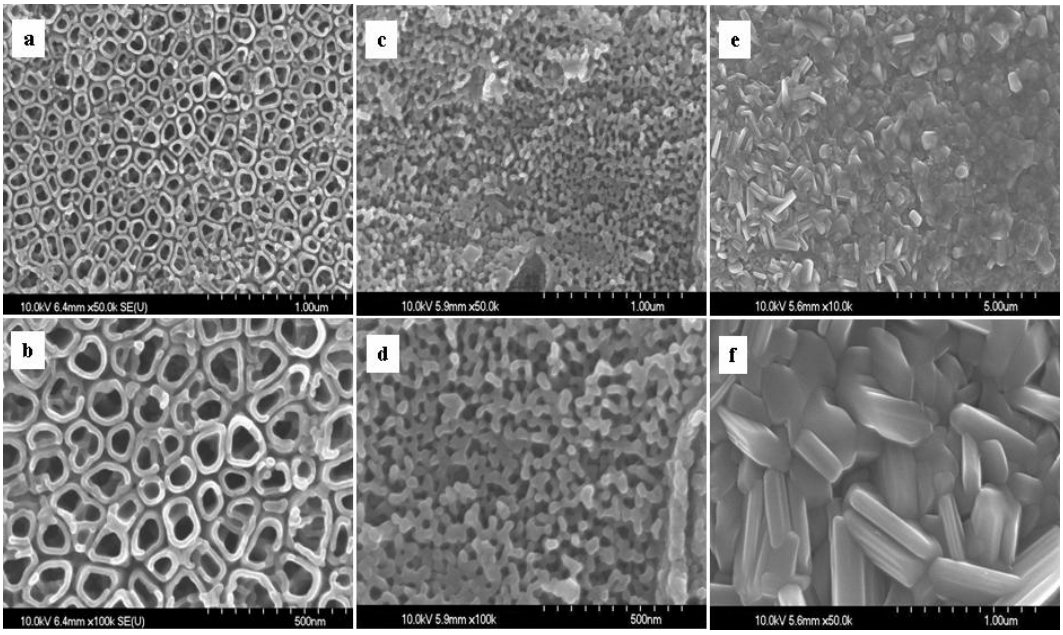

Figure 11. FE-SEM images of nanotube samples (a) 450^{o}C annealed sample with a low magnification (b) high magnification (c) 500^{o}C annealed sample with a low magnification (d) high magnification (e) 600^{o}C annealed sample with a low magnification (f) high magnification

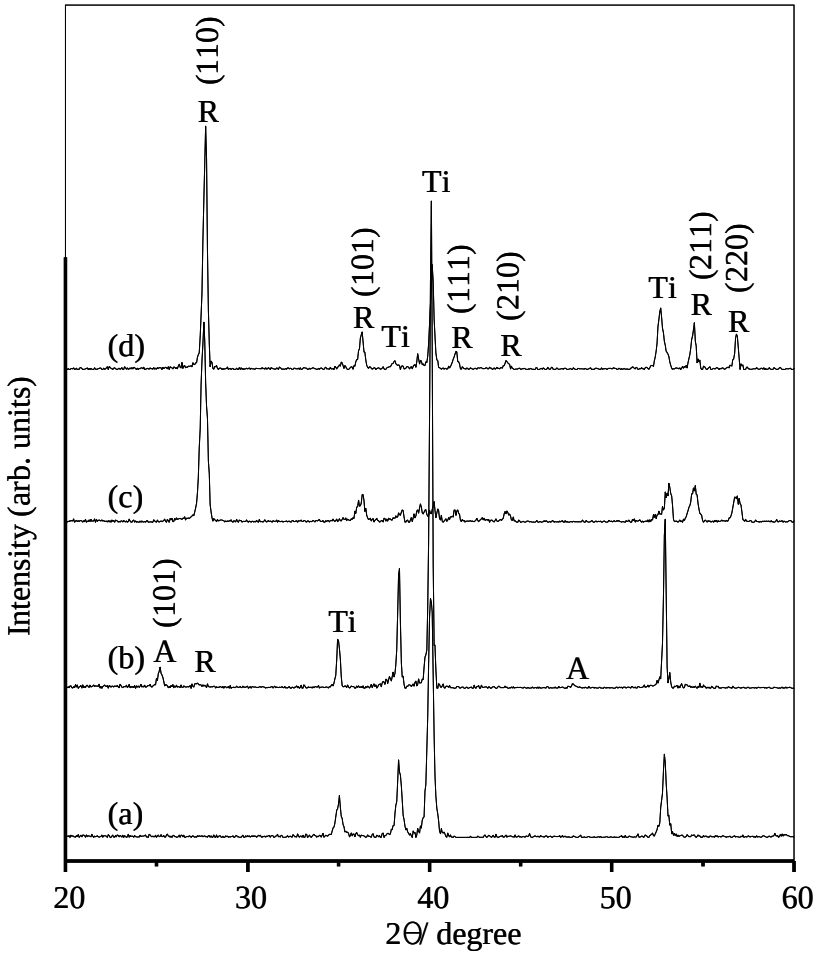

Figure 12. XRD patterns of samples annealed at (a) as prepared sample (b) 450^{o}C (c) 500^{o}C (d) 600^{o}C for 3 h.

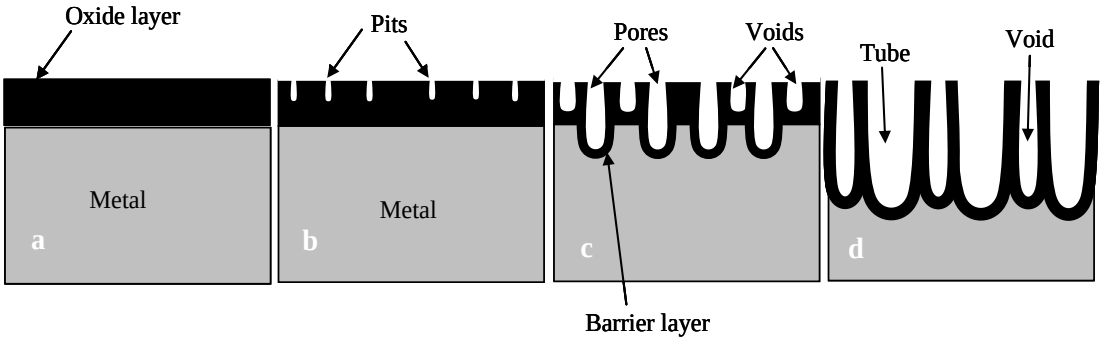

Figure 13. Schematic diagram of nanotubes formation (a) oxide layer formation (b) pit formation on the oxide layer (c) formation of pores between voids with barrier layer at the bottom and (d) fully developed nanotubes

V. The electrochemical behavior and characterization of the anodic oxide film formed on titanium in phosphate buffer media with different pH

The corrosion process is one of the main factors affecting the biocompatibility and mechanical integrity of an implant material. This study examined the anodic oxide films produced on titanium metal using cyclic voltammetric method. The oxide films were produced potentiodynamically at room temperature from a potential ranging from -1.0 to +5.0 V, at a scan rate of $50mVs^{-1}$ in a phosphate buffer solution at pH 2, 7, and 12. After oxide growth, the films were subjected to different repetitive potentiodynamic cycles at $50mVs^{-1}$ between the pre-set cathodic and anodic potentials. The changes in the electrochemical behaviour of the passive electrode, particularly the corrosion of the metal were followed as a function of the electrolyte pH and the number of potentiodynamic cycles. The corrosion of metal surface was severe at pH 2 and increases with increasing number of cycles whereas invariable at pH 7 and in decreasing order at pH 12 as the number of cycle increased. In addition, the surface roughness of modified surfaces was varied as like corrosion of metal as the number of cycles increased.

1. Introduction

Titanium and its alloys are the most popular implant materials in the biomedical field on account of their excellent biocompatibility characteristics such as chemical stability, mechanical resistance and absence of toxicity. The

aerospace and chemical industries are also taking advantage of these characteristics. Corrosion is a critical process in metallic implants because it can adversely affect the biocompatibility and mechanical integrity of a biomaterial. Corrosion and dissolution of the surface film of an implant are two of the most important mechanisms for introducing foreign ions into the body, which can have adverse biological effects [232, 233]. There have been considerable efforts to improve the osseointegration capability of titanium implants by enhancing the level of osteoconduction on their surfaces by modifying the surface morphology and chemistry.

Many surface modification treatments have been studied in an attempt to improve the corrosion behavior of metallic biomaterials, as well as their biocompatibility and mechanical properties [234–236]. Among them, powder/fiber/wire mesh metallurgical sintering [237, 238], plasma spray processing [239, 240], electrochemical oxidation, sol-gel deposition [241], and surface blasting [242] are some methods commonly used to modify the surface topography of load-bearing titanium. Titanium has the characteristics of other valve metals because of its coherent and not easily reducible oxide layer on its surface. In valve metals, the growth of anodic films are commonly irreversible, and occur with a fixed stoichiometry under an electrical field strength and current density described by the high field model: $j=A\exp(\beta\varepsilon)$, where j is the anodic current density, ε is the electric field and A and β are the material dependent constants [243, 244]. On the other hand, the nature of the forming electrolyte solution and its pH also affect the stability, composition and thickness of the anodically grown oxide films [245-248]. The electrochemical

oxidation of titanium has been examined in different electrolytic media using different techniques such as anodization and cyclic voltammetry. During anodic oxidation, different types of titanium oxides (TiO, TiO_2, Ti_2O_3 and Ti_3O_5) may be formed on the titanium surface in which TiO_2 is the most stable and frequently found oxide film [245,249] but the properties of the oxide depend on the method of preparation. Titanium oxide films are usually prepared using an anodic oxidation technique because it is cost effective and oxide formed by this method has good adhesion strength with titanium substrate. However, a voltammetric technique can also be used to form oxide films on valve metals. There are few reports on the production of oxide films using this technique. De Pauli et al. examined the effect of the number of potential cycles on the thin titanium oxide films formed on titanium in Na_2SO_4 solutions at pH 4.0 [250]. Bonilha and Zinolla [251] reported the electrochemical behavior of titanium electrodes in 0.1 mol lit^{-1} KOH in the dark or under UV light. Fast repetitive potentiodynamic cycles were used to examine the potentiodynamic growth and reduction of films. Many studies have reported the changes in the physical properties of valve-metal oxides due to different perturbations occurring during their formation. Blackwood et al [247] investigated the stability of anodic films formed potentiodynamically on titanium in 3 mol lit^{-1} H_2SO_4. Blackwood and Peter [252] also reported the growth stability of anodic oxide films on titanium. Müller et al. [253] examined the stability of the oxide on titanium electrodes in 1 mol lit^{-1} NaOH and in 0.5 mol lit^{-1} H_2SO_4 using potentiodynamic experiments.

This study investigated the anodic films grown potentiodynamically on titanium in a 0.1M phosphate buffer solution at pH 2, 7 and 12, at low voltages and at room temperature. The different repetitive potentiodynamic triangular cycles were applied to the pre-formed anodic oxide.

2. Experimental methods

Commercially pure titanium plates grade 2 (20 × 10 × 2mm) were polished with SiC paper from 220 to 600 grit, ultrasonically cleaned, and dried. Cyclic voltammetry (CV) was performed using a conventional three-electrode cell with a titanium plate as the working electrode, a platinum electrode as the counter electrode and a Ag/AgCl (sat'd. KCl) as the reference electrode. The aqueous phosphate buffer electrolyte solutions were prepared using phosphoric acid and its potassium salts (KH_2PO_4 and K_2HPO_4), at pH of 2, 7 and 12 of concentration 0.1M, respectively.

A commercial potentiostat (EQCM, Shin EQCN1000, and Korea) was used for all electrochemical investigations and the data were recorded using an ECB (model RB 400) X-Y plotter. The anodic oxides were obtained potentiodynamically at scan rate of $50mVs^{-1}$ in the potential range from -1.0 V to +5.0 V. After oxide growth, different repetitive CV cycles (5, 10 and 15) at sweep rate $50mVs^{-1}$ were applied between pre-set cathodic and anodic potentials.

The surface morphology and microstructure were investigated by scanning electron microscopy (SEM, JEOL JSM-5900, Japan) equipped with an Energy Dispersive X-ray Spectrometer (EDS) (Oxford, England). The surface crystalline structure was examined by X-ray diffraction (XRD,

Dmax III-A type, Rigaku Co., Japan) with Cu Kα incident radiation. The surface roughness of the material was measured using a Surftest Formtracer (Surftest SV-402, Mitutoyo Instruments, Tokyo, Japan).

3. Results and discussion

3. 1. Voltammetric study

Titanium electrodes exposed to the atmosphere after mechanical polishing are covered spontaneously by an oxide film. As soon as cyclic voltammetry was performed in phosphate buffer solution at different pH between potentials -1.0 and +5.0 V, the process of dissolution of natural oxide film of TiO_2 begins first. Simultaneously, self-passivated film formation also begins. This potential range was chosen because it encompasses all the electrochemical processes of interest in this work. Figure 14 show the cyclic voltammograms (CV) recorded at 50 mVs^{-1} for titanium oxide growth in phosphate buffer solution at pH 2, 7, and 12, respectively. No changes in the anodic scan were observed. The similarity in the voltammograms at the three different pH is a clear indication that the surface preparation of the electrode and experimental conditions are quite reproducible. A uniform oxide layer begins to form (mainly TiO_2) during anodic oxidation [247, 250, 252, 254], which inhibits the dissolution of titanium according to the following reaction.

$$Ti + 2H_2O \rightarrow TiO_2 + 4H^+ + 4e^- \quad (1)$$

Ti_2O_3 may also be formed [255] but is unstable and rapidly transforms to TiO_2 when it comes in contact with water.

$$Ti_2O_3 + H_2O \rightarrow 2TiO_2 + 2H^+ + 2e^- \quad (2)$$

An anodic current peak can be observed at ≈2.0 V in each case. In the voltammogram obtained after approximately 2.0 V, a slight decrease of anodic current as the potential becomes more positive is noticed, most probably due to a decrease of the real surface area as the film thickness increases. In the lower part of the voltammograms the anodic current rapidly decreases at first, and then decreases slowly to approach zero. The small peaks in the lower part are due to the reduction of a secondary unstable species. Anodic transformations similar to that found for titanium at 2.3 V have also been reported for other valve metals [256, 257]. There has been considerable debate regarding the mechanism for the above phenomenon. Di Quarto et al. [256] attributed this current increase to the start of oxygen evolution when niobium is placed in a sulphuric acid solution, even though no significant oxygen evolution was observed. On the other hand, Schultze and co-workers [258, 259] found quite different oxide growth rates on different single grains of a titanium polycrystalline substrate at potentials > 3 V and also in sulphuric acid solutions. Recently, we reported that the increase in anodic current on passive titanium at 2.0 V might be due to an oxide phase transformation: in aged oxide films that are obtained potentiodynamically up to potentials that more positive than those in the 'hump' region. XRD indicated the presence of a TiO_2 matrix. Systematic studies using other surface techniques are currently underway in an attempt to better understand this phenomenon.

The effect of number of repetitive potentiodynamic cycles on previously grown oxide film was shown in Figure 15. Five different repetitive cycles were carried out at pH 2 solution. After reaching the cathodic potential value of -1.0

V, the sweeps were reversed (made anodic again) and two important features in the potentiodynamic profile of the anodic film were observed. The first is that an anodic peak at approximately 2.0 V is always present, and independent experiments showed that the total charge is dependent on the value of the cathodic potential. This peak has been attributed to the oxidation of hydrogen-containing species that accumulated in the oxide matrix during the cathodic sweep through the hydrogen evolution region [250]. Camara et al. [260] also reported a similar peak for titanium in Na_2SO_4 solutions at various pHs, and interpreted it to be due to the possible oxidation of non-stoichiometric species in the TiO_2 matrix, which had been formed during the cathodic sweep through the hydrogen evolution region. The other important feature drawn from Figure 15 is the continuous increase in anodic current from -1.0 V to +2.0 V with increasing number of potential cycles. The measured anodic current for anodized titanium, in the -1.0 to +5.0 V range, is the sum of two anodic contributions, i.e. one from the reconstruction of the dissolved or reduced oxide during the cathodic excursion and another from the oxygen evolution reaction. Similar profiles were obtained for the other repetitive cycles and pH values. Therefore, the film consists of a crystalline compact layer underlying a hydrous amorphous external layer. Both layers undergo different modifications with the external conditions applied to the passive electrode. The increase in electrical charge with increased electrolyte pH can be seen from the relation between electrical charge and electrolyte pH in Figure 16. This relation is quite linear and shows only one slope. This behavior seems to indicate more electrical charge is needed if the electrolyte pH increases. These results clearly show that

the oxide thickness increases with increasing potential because the charge is directly related to the oxide thickness. Furthermore, this increase is quite linear, which agrees with the growth behavior predicted by the high field growth model [261].

3. 2. Scanning Electron Microscopy

The surface was examined by SEM at different stages of oxidation in order to understand the surface morphology of the anodic oxide film formed on pure titanium metal in phosphate buffer solution. SEM images of the pure titanium samples were taken before electrochemical oxidation to determine the differences in surface morphology after oxidation. After the oxide growth they were subjected to different repetitive CV cycles 5, 10 and 15 between the potentials of -1.0 and +5.0 V in a 0.1M electrolyte solution at different pH, exhibited variations in surface morphology. SEM analysis revealed that the corrosion process was more severe on the titanium surface at pH 2 as the number of cycle increased (Figures 17(a), 17(b) and 17(c)). Uniform corroded surface was seen at higher cycles (Figure 17(c)). This suggests that at low pH, the solution attacks the metal surface quite readily. Titanium in acidic medium, leads corrosion due to destruction of their passivity and loss of mechanical properties. However, at pH 7, there was no any differences in the corrosion of pure titanium regardless of the number of potentiodynamics cycles used (Figures 17(d), 17(e), and 17(f)). This is because there is very slow reaction with metals in a neutral solution. At pH 12, the level of corrosion damage decreased with increasing number of cycles (Figures 17(g), 17(h) and 17(i)). This suggests that at alkaline pH passivation takes place. Passivity is caused by

a change in anodic reaction. The formation of free metal ions gives way to a reaction which forms and insoluble film on the metal surface. These micrographs clearly show the rough passive films with globular morphology. These micrographs also indicate that the intensity of corrosion damage was high at acidic pH and was a function of the number of potentiodynamic cycles. Similarly, the intensity of corrosion damage of titanium was similar at neutral pH and decreases at alkaline pH with increasing number of potentiodynamic cycles.

Table 5 shows surface roughness of different sample groups. Average surface roughness (R_a) was 0.250µm, 0.328µm and 0.407µm for anodized sample at pH 2 , 0.317µm,0.315µm and 0.309µm for anodized sample at pH 7 and 0.278µm,0.214µm and 0.170µm for anodized sample at pH 12 at different repetitive cycles 5,10 and 15, respectively. With comparisons of the roughness of different groups, R_a value showed differences as the electrolyte pH and number of potentiodynamic cycles varied. This shows that the surface roughness of the oxide coating increases with increasing number of repetitive cycles in acidic pH, shows no change regardless of the number of cycles at neutral pH, and decreases at highly alkaline pH. This indicated that average surface roughness (R_a) of anodized sample is a function of electrolyte pH and number of potentiodynamic cycles.

3. 3. X-ray Diffraction

The X-ray diffraction patterns were recorded for pure titanium after CV cycling between potentials of -1.0 V to +5.0 V after a different number of cycles in 0.1M phosphate buffer solutions of pH 2, 7 and 12. Figure 18 (A)

shows intense rutile peak of TiO_2 after 5 cycles but shows only the corresponding peaks of pure titanium at pH 2 after 10 and 15 cycles. This is because at low sweep rates, the degree of order in the films increases substantially. However, at high sweep rates, the rate of dissolution of oxide film may compete with the rate of its formation. At pH 7, the XRD pattern shows only peaks for pure titanium after different repetitive cycles (Figure 18(B)). Similarly, Figure 18 (C) shows the XRD pattern at pH 12. Only the corresponding peaks for pure titanium were observed in all repetitive potentiodynamic cycles. This indicates that the potentiodynamic oxidation reaction after applying an electrical potential at a lower voltage could be beneficial in achieving a higher degree of TiO_2 crystallization. Among them, the TiO_2/Ti film electrode formed at 5.0 V at pH 2 for 5 cycles had the most regular crystal structure of rutile phase. Amorphous titania was formed under the other conditions.

4. Conclusions

The voltammetric experiments have shown the formation of an anodic deposit on titanium anode at three different pH in phosphate buffer solution. SEM micrograph showed that the corrosion of metal increases with increasing the number of cycles at pH 2. The corrosion was more uniform at higher number of cycles. Similarly, there were no changes in the level of corrosion at pH 7 and decreases at pH 12 as the number of potentiodynamic cycles increased. Similar trend was seen in surface roughness. The composition of oxide film consists of rutile TiO_2 after 5 potentiodynamic cycles at pH 2 but in other cases amorphous TiO_2, as shown by the XRD pattern. The results so far

indicate that the corrosion of titanium and surface roughness of modified surface were dependent on electrolyte pH and number of potentiodynamic cycles.

Roughness parameters obtained for Ti electrode in 0.1M phosphate buffer solution with different pH values at different repetitive cycles

Specimen	pH of electrolyte	Repetitive Cycles	Roughness ± SD		
			R_a (μm)	R_y (μm)	R_z (μm)
1	2	5	0.250 ± 0.006	1.751 ± 0.031	1.202 ± 0.007
2	2	10	0.328 ± 0.006	2.194 ± 0.006	1.762 ± 0.006
3	2	15	0.407 ± 0.019	3.400 ± 0.008	1.872 ± 0.041
4	7	5	0.317 ± 0.004	2.088 ± 0.062	1.467 ± 0.005
5	7	10	0.315 ± 0.011	3.023 ± 0.017	1.753 ± 0.005
6	7	15	0.309 ± 0.001	2.124 ± 0.013	1.692 ± 0.002
7	12	5	0.278 ± 0.004	2.248 ± 0.024	1.703 ± 0.008
8	12	10	0.214 ± 0.010	1.999 ± 0.057	1.448 ± 0.017
9	12	15	0.170 ± 0.006	1.981 ± 0.040	1.013 ± 0.094

n=3, SD=Standard Deviation

Table 5. Roughness parameters obtained for Ti electrode in 0.1M phosphate buffer solution with different pH values at different sweep rate

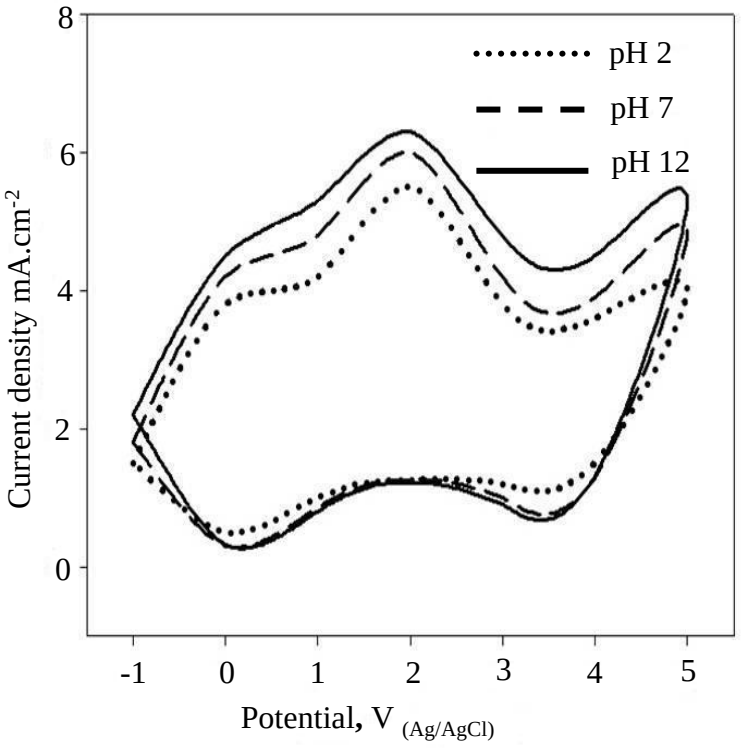

Figure 14. Comparative cyclic voltammograms of the Ti electrode in a phosphate buffer solution at 0.1 Vs^{-1} scan rate at different pH

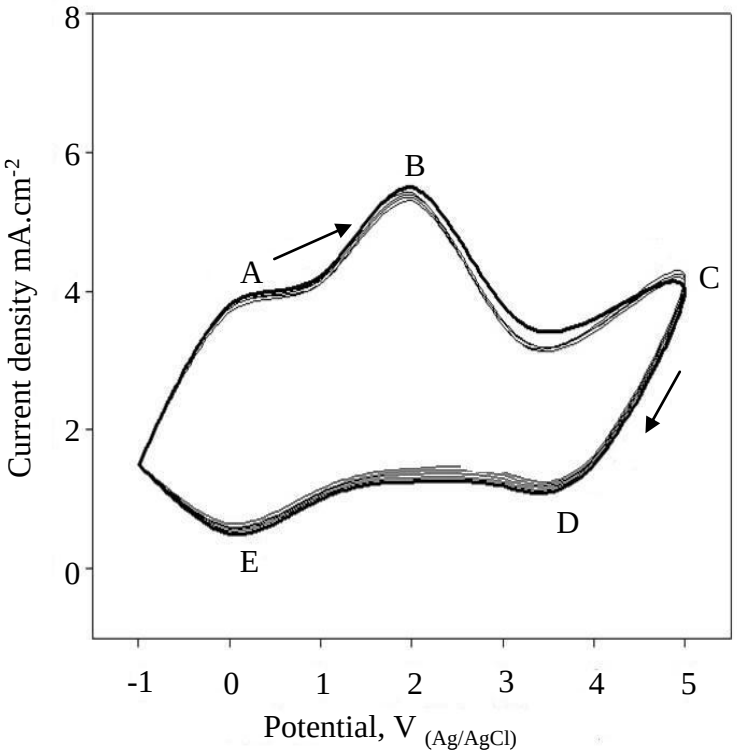

Figure 15. Successive cyclic voltammograms between -1.0 V to 5.0 V, at 50 mV s^{-1}, of a passive Ti electrode in a phosphate buffer solution at pH 2.0, as a function of the number of potential cycles

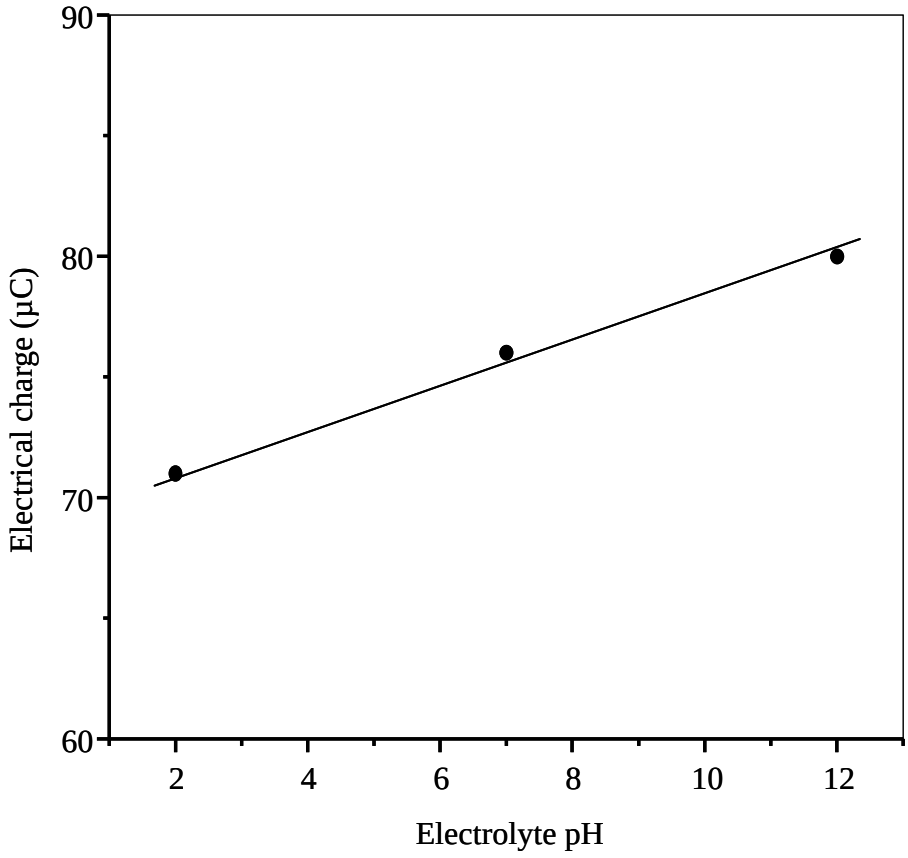

Figure 16. Electrical charge vs. electrolyte pH for cyclic voltammogram obtained in the 0.1M phosphate buffer solution

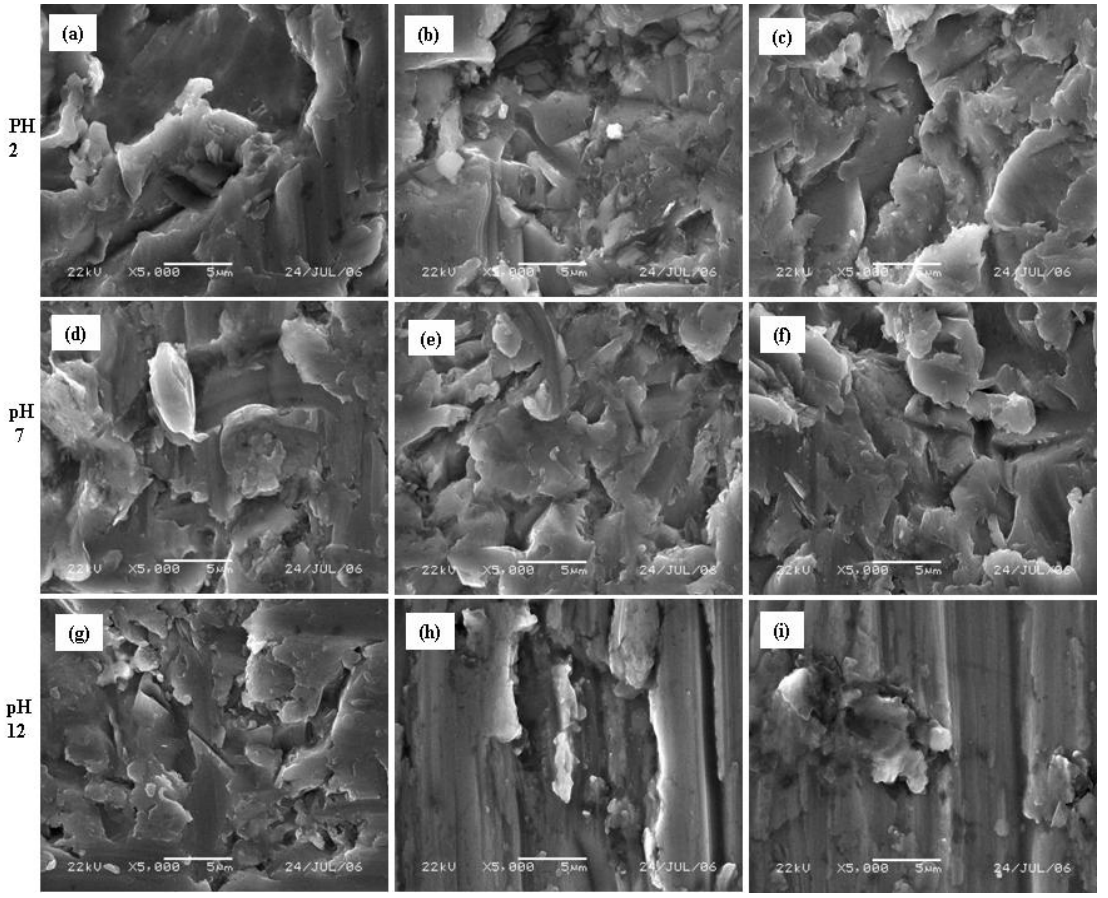

Figure 17. SEM micrographs of the Ti surface in the corroded area in the phosphate buffer solution at different pH and different successive potential cycles, pH 2 (a) 5 (b) 10 (c) 15 cycles, pH 7 (d) 5 (e) 10 (f) 15 cycles, and pH 12 (g) 5 (h) 10 (i) 15 cycles

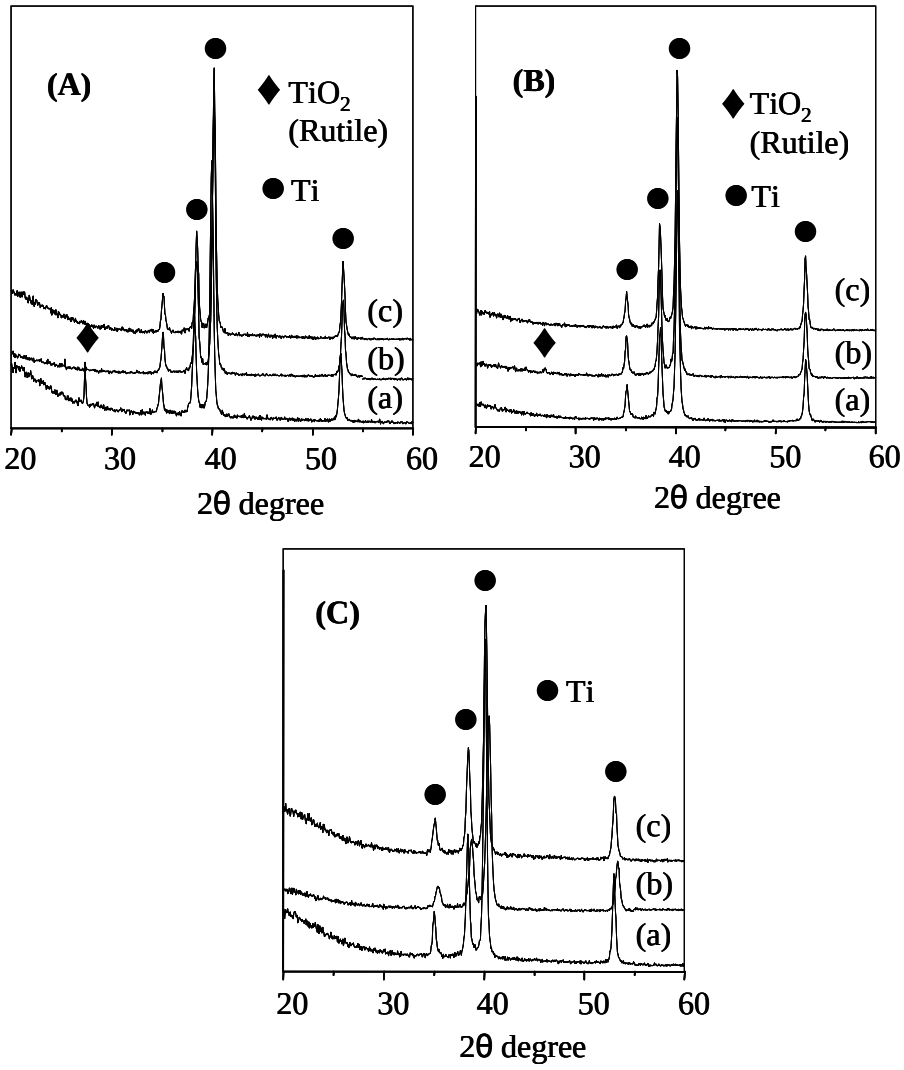

Figure 18. XRD peaks of the specimens treated electrochemically by cyclic voltammetry in phosphate buffer solution and different potential cycles **(A)** pH 2 (a) 5 (b) 10 (c) 15 cycles **(B)** pH 7 (a) 5 (b) 10 (c) 15 cycle **(C)** pH 12 (a) 5 (b) 10 (c) 15 cycles

VI. Summary

In this work, different surface modification methods were used to improve the surface properties (like roughness, structures, energy), mechanical, chemical, and biological properties of titanium for biomedical application. These methods are classified into mechanical, chemical, physical, and combination methods according to the formation mechanism of the modified layer on the surface of titanium. The properties of titanium can be upgraded to some extent after their surfaces are modified using suitable surface modification technology. With the development of the surface engineering, more new surface modification technologies will be introduced to improve the properties of titanium for meeting the clinical needs. The following conclusions were obtained from the above research work.

In chapter II, quenched titanium surface at different temperatures showed variable micromorphology, crystallinity, crystallite size and cellular interactions. Granular oxide at 600^{o}C and 700^{o}C where as large crystallite size were observed at 800^{o}C, 900^{o}C and 1000^{o}C, respectively. High surface roughness and less cell toxicity were obtained with high temperature heating and quenching titanium surface. In chapter III, the electrolyte pH plays important role in governing oxide thickness, composition, degree of crystallinity, and biocompatibility of anodized surface. More uniform porous surface with superior surface roughness was obtained on anodized surface at pH 12. Incorporation of P ions on oxide film increase as the electrolyte pH decrease. Superior biocompatibility result was obtained at higher pH anodized titanium. Chapter IV illustrated that just prepared nanotube film is amorphous.

Anatase appeared at heating the sample at 450^{o}C. Nanotubes completely coalesced with complete transformation of anatase to rutile phase at 500^{o}C. Similarly, as temperature increase dense rutile crystals were obtained with intense crystallinity. Chapter V highlights the corrosion of titanium metal surface at different electrolyte pH. Sever corrosion of metal was observed at low electrolyte pH (acidic electrolyte). Uniform corrosion at neutral pH and corrosion decreases at alkaline pH as the number of repetitive potential cycles increase on previously formed oxide film. Also the surface roughness of modified surface depends on similar trend as corrosion. In conclusion, it is expected that the titanium modified by above methods is available in application to the dental as well as orthopedic implant system.

References

1. B. D. Ratner, and A. S. Hoffman, Biomaterials Science: An Introduction to Materials in Medicine. California: Academic Press, Inc., 1996, Chapter 2, 37-131.
2. J. Walczak, F. Shahgaldi, and F. Heatley, Biomaterials1998; 19: 229-237.
3. M-F. Harmand, Journal of Biomaterial Science, Polymer Edition 1994; 6 (9): 809-814.
4. S. A. Brown, K. Zhang, K. Merritt, and J. H. Payer, Journal of Biomedical Materials Research 1993; 27: 1007-1017.
5. O. E. M. Pohler, "Failures of Metallic Orthopedic Implants." Metals Handbook. Ninth Edition. American Society for Metals. Metals Parks: ASM International 1986; 11: 668-694.
6. R. T. Bothe, K. E. Beaton, and H. A. Davenport, Surg. Gynecol. Obstet. 940 ; 71: 598-602.
7. T. Albrektsson, The response of bone to titanium implants. CRC Crit Rev Biocompatibility 1985; 1: 53-84.
8. T. Eliades, Int J Oral Maxillofac Implants 1997; 12: 621-627.
9. J. C. Keller, C. M. Stanford, J. P. Wightman, R. A. Draughn, and R. Zaharis, J Biomed Mater Res 1994; 28: 939-946.
10. P. I. Branemark, Introduction to osseointegration. In: Branemark PI, Zarb GA, Albrektsson T, eds. Tissue-integrated prostheses. Quintessence Publishing Co. Inc., Chicago. 1985; 11-76.

11. P. Ducheyne, J Oral Implantol 1988; 14: 325-340.
12. T. G. Donley, and W. B. Gillette, J Periodontol 1991; 62: 153-160.
13. K. E. Healy, and P. Ducheyne, J Biomed Mater Res 1992; 26: 319-338.
14. R. M. Pilla, and G. C. Weatherlz, Developments in implant alloys. CRC Crit Rev Biocompatibility1986; 1: 371-403.
15. E. P. Lautenschlager, and P. Monaghan, Int Dent J 1993; 43: 245-253.
16. J. Lausmaa, B. Kasemo, H. Mattsson, and H. Odelius, Appl Surface Sci 1990; 45: 189-200.
17. M. Ask, J. Lausmaa, and B. Kasemo, Appl Surface Sci 1988-1989; 35: 283-301.
18. B. Kasemo, and J. Lausmaa, Int J Oral Maxillofac Implant 1988; 3: 247-259.
19. M. C. Garcia-Alonso, L. Saldana, G. Valles, J. L. Gonzalez-Carrasco, J.Gonzalez-Cabrero, M. E. Martinez, E. Gil-Garay, and L. Munuera, Biomaterials 2003; 24, 19-26.
20. L. Postiglione, G. D. Domenico, L. Ramaglia, S. Montagnani, S. Salzano, F. D. Meglio, L. Sbordone, M. Vitale, and G. Rossi, J Dent Res 2003; 82: 692-696.
21. K. Mustafa, A. Wennerberg, J. Wroblewski, K. Hultenby, B. S. Lopez, and K. Arvidson, Clin Oral Impl Res 2001; 12: 515-525.

22. K. T. Bowers, J. C. Keller, B. A. Randolph, D. G. Wick, and C. M. Michaels, Int J Oral Maxillofac Implants 1992; 7: 302-310.
23. N. Lumbikanonda, and R. Sammons, Int J Oral Maxillofac Implants 2001; 16: 627-636.
24. Y. Shibata, M. Hosaka, H. Kawai, and T. Miyazaki, Int J Oral Maxillofac Implants. 2002; 17(6): 771-777.
25. R. A. Buchanan, E. D. Rigney Jr, and J. M. Williams, J Biomed Mater Res. 1987; 21: 355-366.
26. R. A. Buchanan, I. S. Lee, and J. M. Williams, J Biomed Mater Res.1990; 4 : 309-318.
27. A. M. Maurer, S. A. Brown, J. H. Payer, K. Merritt, and J. S. Kawalec, J Orthop Res. 1993; 11: 865-873.
28. M. A. De Maeztu, J. I. Alava, and C. Gay-Escoda, Clin Oral Implants Res. 2003; 14: 57-62.
29. M. C. García-Alonso, L. Saldaña, G. Vallés, J. L. González-Carrasco, J. González-Cabrero, M. E. Martínez, E. Gil-Garay, and L. Munuera, Biomaterials 2003; 24: 19-26.
30. B. Feng, J. Weng, B. C. Yang, S. X. Qu, and X. D. Zhang, Biomaterials 2003; 24: 4663-4670.
31. B. Feng, J. Weng, B. C. Yang, S. X. Qu, and X. D. Zhang, Biomaterials 2004; 25: 3421-3428.

32. A. P. Ameen, R. D. Short, R. Johns, and G. Schwach, Clin Oral Implants Res. 1993; 4:144-150.
33. M. Takeuchi, Y. Abe, Y. Yoshida, Y. Nakayama, M. Okazaki, and Y. Akagawa, Biomaterials 2003; 24:1821-1827.
34. I. Degasne, M. F. Basle, V. Demain, G. Hure, M. Lesourd, B. Grolleau, L. Mercier, and D. Chappard, Calcif Tissue Int 1999; 64: 499-507.
35. K. Kieswetter, Z. Schwartz, T. W. Hummert, D. L. Cochran, J. Simpson, and D. D. Dean, J Biomed Mater Res 1996; 32: 55-63.
36. C. Viornery, H. L. Guenther, B. O. Aronsson, P. Pechy, P. Descouts, and M. Gratzel, J Biomed Mater Res. 2002; 62: 149-155.
37. K. De Groot, R. G. T. Geesink, C. P. A. T. Klein, and P. Serekion, J Biomed Mater Res 1987; 21: 1375-1381.
38. J. D. de Brujin, C. P. A. T. Klein, K. de Groot, and C. A. van Bitterswijk, J Biomed Mater Res 1992; 26: 1365-1382.
39. P. A. Ramires, A. Romito, F. Cosentino, and E. Milella, Biomaterials 2001; 22: 1467-1474.
40. C. Massaro, M. A. Baker, F. Cosentino, P. A. Ramires, S. Klose, and E. Milella, J Biomed Mater Res 2001; 58(6): 651-657.
41. H. W. Kim, Y. H. Koh, L. H. Li, S. Lee, and H. E. Kim, Biomaterials 2004; 25: 2533-2538.
42. I. M. O. Kangasniemi, C. C. P. M. Verheyen, E. A. van der Velde, and K. de Groot, J Biomed Mater Res 1994; 28: 563-572.

43. M. D. Ball, S. Downes, C. A. Scotchford, E. N. Antonov, V. N. Bagratashvili, V. K. Popov, W. J. Lo, D. M. Grant, and S. M. Howdle, Biomaterials 2001; 22: 337-347.
44. M. Yoshinari, B. Klinge, and T. Derand, Clin Oral Implants Res 1996; 7(2): 96-100.
45. F. Z. Cui, Z. S. Lout, and Q. Feng, J Mater Sci Mater Med 1997; 8: 403-405.
46. Y. C. Jung, C. H. Han, I. S. Lee, and H. E. Kim, Int J Oral Maxillofac Implants. 2001; 16(6): 809-818.
47. H. Ishizawa, M. Fujino, and M. Ogino, J Biomed Mater Res 1995; 29: 1459-1468.
48. H. Ishizawa, and M. Ogino, J Biomed Mater Res 1995; 29: 1071-1079.
49. H. Ishizawa, M. Fujino, and M. Ogino, J Biomed Mater Res 1997; 35: 199-206.
50. J. Y. Suh, B. C. Jang, X. L. Zhu, J. L. Ong, and K. Kim, Biomaterials 2003; 24: 347-355.
51. L. Gineste, M. Gineste, X. Ranz, A. Ellefterion, A. Guilhen, N. Ronquet, and P. Frayssinet, J Biomed Mater Res (Appl Biomater) 1999; 48: 224-234.
52. L. Montanaro, C. R. Arciola, D. Campoccia, and M. Cervellati, Biomaterials 2002; 23: 3651-3659.
53. K. Okamoto, T. Matsuura, R. Hosokawa, and Y. Akagawa, J Dent Res 1998; 77: 481-487.

54. T. Matsuura, R. Hosokawa, K. Okamoto, T. Kimoto, and Y. Akagawa, Biomaterials 2000; 21: 1121-1127.

55. S. Tosatti, S. M. De Paul, A. Askendal, S. VandeVondele, J. A. Hubbell, P. Tengvall, and M. Textor, Biomaterials 2003; 24: 4949-4958.

56. J. D. Bumgardner, R. Wiser, S. H. Elder, R. Jouett, Y. Yang, and J. L. Ong, J Biomater Sci Polymer Edn 2003; 14(12): 1401-1409.

57. M. M. Bornstein, A. Lussi, B. Schmid, U. C. Balder, and D. Buser, Int J Oral Maxillofac Implants. 2003; 18: 659-666.

58. S. Szmukler-Moncler, D. Perrin, V. Ahossi, G. Magnin, and J. P. Bernard, J Biomed Mater Res. 2004; 68B: 149-159.

59. S. Guizzardi, C. Galli, D. Martini, S. Belletti, A. Tinti, M. Raspanti, P. Taddei, A. Ruggeri, and R. Scandroglio, J Periodontol. 2004; 75: 273-282.

60. C. Larsson, P. Thomsen, J. Lausmaa, M. Rodahl, B. Kasemo, and L. E. Ericson, Biomaterials 1994; 15: 1062-1074.

61. N. Kanematu, K. I. Shibata, S. Kurenuma, K. Watanabe, A. Yamagami, Y. Nishio, and T. Fujii, J Gifu Dent Soc 1990; 17: 583-591.

62. M. Fini, A. Cigada, G. Rondelli, R. Chiesa, R. Giardino, G. Giavaresi, N. N. Aldini, P. Torricelli, and B. Vicentini, Biomaterials 1999; 20: 1587-1594.

63. Y. T. Sul, C. B. Johansson, Y. Jeong, A. Wennerberg, and T. Albrektsson, Clin Oral Impl Res 2002; 13:252-259.

64. X. L. Zhu, K. Kim, J. L. Ong, and Y. Jeong, Int J Oral Maxillofac Implants 2002; 17: 331-336.

65. J. L. Delplancke, and R. Winand, Electrochim. Acta 1988; 33: 1539-1549.
66. T. Shibata, and Y.C. Zhu, Corros. Sci. 1995; 37: 253-270.
67. X. L. Zhu, K. H. Kim, and Y. Jeong, Biomaterials 2001; 22: 2199-2206.
68. E. De Giglio, L. Sabbatini, S. Colucci, and G. Zambonin, J Biomater Sci Polymer Edn 2000; 11: 1073-1083.
69. W. C. Hueper, J Net Cancer Inst 1955; 16: 55-73.
70. A. McDugall, J Bone Joint Surg 1956; 38-B: 709-713.
71. G. Kanzatzis, Environ Health Pers 1981; 40:143-161.
72. G. Magmusson, M. Bergman, B. Bergman, and R. Soremark, Scand J Dent Res 1982; 90: 163-167.
73. G. Wang, and X. Cheng, Zhonghua Kou Qiang Yi Xue Za Zhi 2001; 36: 427-430.
74. W. W. Son, X. Zhu, H. I. Shin, J. L. Ong, and K. H. Kim, J Biomed Mater Res. 2003; 66B: 520-525.
75. K. Kieswetter, Z. Schwartz, D. D. Dean, and B. D. Boyan, Crit Rev Oral Biol Med 1996; 7: 329-345.
76. B. Lassen, K. Holmberg, C. Brink, A. Carlen, and J. Olsson, Colloid Polym Sci 1994; 272: 1143-1150.
77. S. Welin-Klingström, A. Askendal, and H. Elwing, J Colloid Interface Sci 1993; 158: 188-194.
78. K. Bergström, E. Österberg, K. Holmberg, A. S. Hoffman, T. P. Schuman, A. Kozlovsky, and J. H. Harris, J Biomater Sci Polym Ed 1994; 6: 123-132.
79. N. J. Hallab, K. J. Bundy, K. O'connor, R. L. Moses, and J. J. Jacobs, Tissue Engineering 2001; 7: 55-71.

80. A. Arys, C. Philippart, N. Dourov, Y. He, Q. T. Le, and J. J. Pireaux, J Biomed Mater Res 1998; 43: 300-312.

81. A. Wennerberg, P. Bolind, and T. Albrektsson, Swed Dent J1991; 15: 95-101.

82. L. V. Carlsson, T. Alberktsson, and C. Berman, Int J Oral Maxillofac Implants 1989; 4: 199-204.

83. D. Buser, R. K. Schenk, S. Steinemann, J. P. Fiorellini, C. H. Fox, and H. Stich, J Biomed Mater Res 1991; 25: 889-902.

84. A. S. G. Curtis, and P. Clark, Crit Rev Biocomp 1990; 5: 343-362.

85. A. Wennerberg, T. Albrektsson, B. Andersson, and J. J. Krol, Clin Oral Implants Res 1995; 6: 24-30.

86. K. T. Bowers, J. C. Keller, B. A. Randolph, D. G. Wick, and C. M. Michaels, Int J Oral Maxillofac Implants 1992; 7: 302-310.

87. D. Cochran, J. Simpson, H. Weber, and D. Buser, Int J Oral Maxillofac Implants 1994; 9, 289-297.

88. F. Grinell, Int Rev Cytol 1978; 53: 65-144.

89. B. S. Pearson, R. J. Klebe, B. D. Boyan, and D. Moskowicz, J Dent Res 1988; 67: 515-517.

90. R. E. Weiss, and A. H. Reddi, J Cell Biol 1981; 88: 630-636.

91. K. Anselme, M. Bigerelle, B. Noel, E. Dufresne, D. Judas, A. Iost, and P. Hardouin, J Biomed Mater Res 2000; 49: 155-166.

92. K. Kieswetter, Z. Schwartz, T. W. Hummert, D. L. Cochran, J. Simpson, D. D. Dean, and B. D. Boyan, J Biomed Mater Res 1996; 32: 55-63.

93. B. D. Boyan, J. Lincks, C. H. Lohmann, V. L. Sylvia, K. L. Cochran, C. R. Blanchard, and D. D. Dean, and Z. Schwart, Journal of Orthopedic Research 1999; 17: 446-457.

94. J. Y. Martin, Z. Schwartz, T. W. Hummert, D. M. Schraub, J. Simpson, J. Jr. Lankford, D. D. Dean, D. L. Cochran, and B. D. Boyan, J Biomed Mater Res1995; 29: 389-401.

95. I. Degasne, M. E. Basle, V. Demais, G. Hure, M. Lesourd, B. Grolleau, L. Mercier, and D. Chappard, Calcif Tissue Int 1999; 64: 499-507.

96. K. A. Thomas, and S. D. Cook, J Biomed Mater Res 1985; 19: 875-901.

97. B. Chehroudi, T. R. Gould, and D. M. Brunette, J Biomed Mater Res 1991; 25: 387-405.

98. G. Hure, K. Donath, M. Lesourd, D. Chappard, and M. F. Basle, Int J Oral Maxillofac Implants 1996; 11: 506-511.

99. A. Curtis, and C. Wilkinson, Biomaterials 1997; 18: 1573-1583.

100. C. D. W. Wilkinson, A. S. G. Curtis, and J. Crossan, J Vac Sci Technol 1998; B16: 3132-3136.

101. P. Clark, P. Connolly, and A. S. Curtis, Development 1990; 108: 635-644.

102. B. Chehroudi, T. R. L. Gould, and D. M. Brunette, J Biomed Mater Res 1989; 23: 1067-1085.

103. E. T. den Braber, H. V. Jansen, M. J. de Boer, H. J. Croes, M. Elwenspoek, L. A. Ginsel, and J. A. Jansen, J Biomed Mater Res 1998; 40: 425-433.

104. E. T. den Braber, J. E. de Ruijter, L. A. Ginsel, A. F. von Recum, and Jansen, J Biomed Mater Res 1998; 40: 291-300.
105. K. D. Chesmel, C. C. Clark, C. T. Brighton, and J. Black, J Biomed Mater Res 1995; 29: 1101-1110.
106. B. Wojciak-Stothard, Z. Madeja, W. Korohoda, A. Curtis, and C. Wilkinson, Cell Biol Int 1995; 19: 485-490.
107. X. F. Walboomers, H. J. E. Croes, L. A. Ginsel, and J. A. Jansen, J Biomed Mater Res 1999; 47: 204-212.
108. C. E. Cambell, and A. F. Von Recum, J Invest Surg 1989; 2: 51-74.
109. X. F. Walboomers, L. A. Ginsel, and J. A. Jansen, J Biomed Mater Res 2000; 51: 529-534.
110. T. Albrektsson, J Oral Maxillofac Surg 1998; 56: 1312-1326.
111. L. L. Hench, Bioceramics. J Am Ceram Soc 1998; 81:1705-1728.
112. J. C. Keller, C. M. Stanford, J. P. Wightman, R. A. Draughn, and R. Zaharias, J Biomed Mater Res 1994; 28: 939-946.
113. J. Li, H. Liao, B. Fantasy, L. Hermannsson, and T. Johnsson, Biomaterials 1997; 18: 691-696.
114. K. Anselme, M. Bigerelle, B. Noel, A. Iost, P. Hardouin, J Biomed Mater Res 2002; 60: 529-540.
115. R. Stangl, B. Rinne, S. Kastl, and C. Hendrich, European Cells and Materials 2001; 2: 1-9.
116. J. J. Klawitter, and S. F. Hulbert, J Biomed Mater Res 1971; 2: 161-229.
117. C. A. Homsy, Orthop Clin North Am 1973; 4: 295-311.
118. R. M. Pilliar, Implant Dent 1998; 7: 305-314.

119. H. Nakahara, V. M. Goldberg, and A. I. Kaplan, Clin Orthop Rel Res 1992; 276: 291-298.
120. J. Tomes, and C. de Morgan, Phil. Trans. Roy. Soc. 1853; 143: 109-139.
121. M. Noda, and J. J. Camilliere, Endocrinology 1989; 124: 2991-2994.
122. J. W. Chow, A. J. Wilson, T. J. Chambers, and S. W. Fox, J Bone Miner Res 1998; 13:1760-1767.
123. N. M. Hancox, Cambridge University Press 1972: p 63-105.
124. R. J. Freshney, Culture of animal cells: a manual of basic technique. John Wiley & Sons, INC., Second Edition 1987: 249-256.
125. A. B. Ferguson, P. G. Laing, and E. S. Hodge, J Bone Joint Surg 1960; 42-A: 77-90.
126. T. Inoue, M. Shimono, Y. Abiko, and T. Kaku, Bull of Kanagawa Dent Col 1994; 22: 125-137.
127. G. Schneider, and K. Burridge, Exper Cell Res 1994; 214: 264-269.
128. R. Rajaraman, D. E. Rounds, S. P. S. Yen, and A. Rembaum, Exp Cell Res 1974; 88: 327-399.
129. J. E. Ellingsen, Biomaterials 1991; 12: 593-596.
130. C. R. Howlett, M. D. M. Evans, W. R. Walsh, G. Johnson, and J. G. Steele, Biomaterials 1994; 15: 213-222.
131. C. M. Michaels, J. C. Keller, C. M. Stanford, M. Solursh, and C. Mackenzie, J Dent Res1989; 68: 276.
132. A. L. Rosa, and M. M. Beloti. Braz Dent J 2003; 14: 16-21.
133. C. M. Stanford, J. C. Keller, and M. Solursh, J Dent Res 1994; 73: 1061-1071.

134. J. Y. Martin, D. D. Dean, D. L. Cochran, J. Simpson, B. D. Boyan, and Z. Schwartz, Clin Oral Impl Res 1996; 7: 27-37.

135. F. A. Akin, H. Zreiqat, S. Jordan, M. B. J. Wijesundara, and L. Hanley, J Biomed Mater Res 2001; 57: 588-596.

136. J. B. Park, Biomaterials science and engineering, Plenum Press, New York 1989.

137. D. C. Mears, Materials and orthopedics surgery, Baltimore, MD: Williams and Wilkins 1979.

138. D. M. Brunette, P. Tengvall, M. Textor, and P. Thomsen, Titanium in medicine, Springer, NewYork 2001.

139. S. G. Steinemann, Periodontology 2000 1998; 17: 7-21.

140. M. Jobin, M. Taborelli, and P. Descouts, J. Appl. Phys. 1995; 77: 5149-5155.

141. T. M. Lee, E. Chang, Y. C. Yang, J. Mater. Sci.: Mater. Med. 1998; 9: 439-448.

142. P. Ducheyne, and K. E. Healy, J. Biomed. Mater. Res. 1988; 22: 1137-1163.

143. J. Chen, W. Tong, Y. Cao, J. Feng, and X. Zhang, J Biomed Mater Res 1997; 34: 15-20.

144. R. V. Dijk, H.G. Schaeken, J. C. G. Wolke, H. M.C. Marée, F. H. P. M. Habraken, J. Verhoeven, and J.A. Jansen, J Biomed Mater Res 1995; 29: 269-276.

145. L. Jonášová, F. A. Müller, A. Helebrant, J. Strnad, and P. Greil, Biomaterials 2004; 25: 1187-1194.

146. F. Xiao, K. Tsuru, S. Hayakawa, and A. Osaka, Thin Solid Films 2003; 441: 271-276.

147. J. M.Wu, S. Hayakawa, K. Tsuru, and A. Osaka, Scripta Mater 2002; 46: 101-106.

148. S. Fujibayashi, M. Neo, H. M. Kim, T. Kokubo, and T. Nakamura, Biomaterials 2004; 25: 443-450.

149. Y. T. Sul, C. B. Johansson, Y. Jeong, and T. Albrektsson, Med Eng Phys 2001; 23: 329-346.

150. B. Yang, M. Uchida, H. M. Kim, X. Zhang, and T. Kokubo, Biomaterials 2004; 25: 1003-1010.

151. C. A. Babbush, J. N. Kent, and D. J. Misiek, J. Oral. Maxillofac. Surg. 1986; 44: 274-282.

152. A. Wennerberg, T. Albrektsson, C. Johansson, and B. Andersson, Biomaterials 1996; 17: 15-22.

153. A. Gaggl, G. Schultes, W. D. Müller, and H. Kärcher, Biomaterials 2000; 21: 1067-1073.

154. B. Feng, J. Y. Chen, S. K. Qi, L. He, J. Z. Zhao, and X. D. Zhang, J. Mater. Sci. Mater. Med. 2002; 13: 457- 464.

155. J. R. Birch, and T. D. Burleigh, Corrosion 2000; 56(12): 1233-1241.

156. E. Hristova, L. Arsov, B.N. Popav, and R.E. White, J. Electrochem. Soc. 1997; 144: 2318-2323.

157. Y. T. Sul, C. B. Johansson, S. Petronis, A. Krozer, Y. S. Jeong, A. Wennerberg, and T. Albrektsson, Biomaterials 2002; 23: 491-501.

158. P. Li, I. Kangasniemi, K. De Groot, and T. Kokubo, J. Am. Ceram. Soc. 1994; 77: 1307-1312.

159. N. N. Dinh, N. Th. T. Oanh, P. D. Long, M. C. Bernard, and A. Hugot-Le Goff, Thin Solid Films 2003; 423: 70-76.

160. L. S. Hsu, R. Rujikorakarn, J. R. Sites, and C. Y. She, J. Appl. Phys. 1986; 59: 3475-3480.

161. T. Albrektsson, CRC Critical Reviews in Biocompatibility 1984; 1: 53-84.

162. L. J. Alemany, M. A. Bańares, E. Pardo, F. Martín-Jiménez, and J. M. Blasco, Mater. Charact. 2000; 44: 271-275.

163. P. Ducheyne and G. W. Hastings, "Metal and ceramic biomaterials", CRC Press Inc., Boca Raton 1984.

164. Brooks C. R., "Titanium based alloys in: Heat treatment, structure and properties of nonferrous alloys", p. 329, American Society for Metals 1982.

165. H. H. Afify, S. A. Mahmoud and A. Ashour, Thin Solid Films 1995; 263: 248-251.

166. R. C. Weast (ed.) in "CRC Hand Book of Chemistry and Physics. 70th edition, 1989-1990", (CRC Press Inc., Boca Raton, Florida, D-90).

167. P. A. Lee, K. F. Stork, B. L. Maschhoff, K. W. Nebesny, and N. R. Armstrong, Surf. Interf. Analy.1991; 17: 48-56.

168. B. F. Lowenberg, S. Lugowski, M. Chirman, and J. E. Davis, J. Mater. Sci. Mater. Med. 1994; 5: 467-472.

169. B. W. Callen, B. F. Lowenberg, S. Lugowski, R. N. S. Sodi, and J. E. Davis, J Biomed Mater Res 1995; 29: 279-290.

170. J. M. Pan, B. L. Maschhoff, U. Diehold, and T. E. Madey, J.Vac. Sci. Technol. A 1992; 10: 2470-2476.

171. J. B. Park, and R. S. Lakes, "Biomaterials: An introduction", p 89, Plenum Press, New York 1992.

172. S. G. Steinemann, Periodontology 2000 1998; 17: 7-21.

173. B. Kasemo, and J. Lausmaa, Surface science aspects on inorganic biomaterials. In CRC Critical Reviews in Biocompatibility, Williams F, Ed.; CRC Press: New York 1986; 2: 335-380.

174. D. Buser, R. K. Schenk, S. Steinemann, J. P. Fiorellini, C. H. Fox, and H. Stich, J. Biomed. Mater. Res. 1991; 25: 889-902.

175. C. Larsson, P. Thomsen, J. Lausmaa, M. Rodahl, B. Kasemo, and E. Ericson, Biomaterials 1994; 15: 1062-1074.

176. Z. Schwartz, J. Y. Martin, D. D. Dean, J. Simpson, D. L. Cochran, and B. D. Boyan, J. Biomed. Mater. Res.1998; 30: 145-155.

177. D. L. Cochran, R. K. Schenk, A. Lussi, F. L. Higginbot tom, and D. Buser, J. Biomed. Mater. Res.1998; 40: 1-11.

178. I. Degasne, M. F. Basle, V. Demais, G. Hure, M. Lesourd, B. Grolleau, L. Mercier, and D. Chappard, Calcif. Tissue Int. 1999; 64: 499-507.

179. J. G. Yu, X. J. Zhao, and Q. N. Zhao, Mater. Chem. Phys. 2001; 69: 25-29.

180. X. H. Wang, F. Zhang, C. R. Li, Z. H. Zheng, X. Wang, X. H. Liu, A. Chen, and Z. B. Ziang, Surf. Coat. Technol. 2000; 128-129: 36-42.

181. K. van Dijk, H. G. Schaeken, J. C. G. Wolke, C. H. M. Marée, F. H. P. M. Habraken, J. Verhoeven, and J. A. Jansen, J. Biomed. Mater. Res. 1995; 29: 269-276.

182. P. R. Klokkevold, R. D. Nishimura, M. Adachi, and A. Caputo, Clin. Oral Implants Res. 1997; 8: 442-447.

183. Y. C. Zhu, and C. X. Ding, J. Eur. Ceram. Soc. 2000; 20: 127-132.

184. D. H. Kohn, Curr. Opin. Solid State Mater. Sci.1998; 3: 309-316.

185. I. M. O. Kangasniemi, C. C. P. M. Verheyen, E. A. van der Velde, and K. De Groot, J. Biomed. Mater. Res. 1994; 28: 563-572.

186. A. L. Yerokhin, X. Nie, A. Leyland, A. Matthews, and S. J. Dowey, Surf. Coat. Technol. 1999; 122: 73-93.

187. Y. Han, and K. Xu, J. Biomed. Mater. Res. 2004; 71A: 608-614.

188. W. H. Song, J. K. Jun, Y. Han, and S. H. Hong, Biomaterials 2004; 25: 3341-3349.

189. D. S. Dunn, S. Raghavan, and R. G. Volz, J. Biomed. Mater. Res. 1993; 27: 895-900.

190. J. L. Delplancke, and R. Winand, Electrochim. Acta 1988; 33: 1551-1559.

191. T. Shibata, and Y. C. Zhu, Corrosion Science 1995; 37: 133-144.

192. M. P. Pedeferri, B. Del Curto, and P. Pedeferri, Proceedings of Passivity-9, Paris 2005.

193. A. L. Yerokhin, X. Nie, A. Leyland, and A. Matthews, Surf. Coat. Technol. 2000; 130: 195-206.

194. X. Nie, A. Leyland, A. Matthews, J. C. Jiang, and E. I. Meletis, J Biomed Mater Res 2001; 57: 612-618.
195. M. V. Diamanti, and M. P. Pedeferri, Corrosion Science 2007; 49: 939-948.
196. X. Nie, E. I. Meletis, J. C. Jiang, A. Leyland, A. L. Yerokhin, and A. Matthews, Yerokhin AL, Matthews A. Surf. Coat. Technol. 2002; 149: 245-251.
197. R. Beranek, H. Hildebrand, and P. Schmuki, Electrochem. Solid State Lett. 2003; 6: B12-B14.
198. J. M. Macak, K. Sirotna, and P. Schmuki, Electrochim. Acta 2005; 50: 3679-3684.
199. J. M. Macak, H. Tsuchiya, and P. Schmuki, Angew. Chem. Int. Ed. 2005; 44: 2100-2102.
200. Y. T. Sul, C. B. Johansson, Y. Jeong, and T. Albrektsson, Med Eng Phys 2001; 23: 329-346.
201. T. Hanawa, and M. Ota, Biomaterials 1991; 12: 767-774.
202. H. Ishizawa, and M. Ogino, J Biomed Mater Res 1995; 29: 1071-1079.
203. J. Choi, R. B. Wehrspohn, J. Lee, and U. Gösele, Electrochim. Acta 2004; 49: 2645-2652.
204. J. S. L. Leach, and B. R. Pearson, Corrosion Science 1988; 28: 43-56.
205. J. Cl. Puippe, European Cells and Materials 2003; 5: 32-33.
206. T. Hanawa, Mater Sci Eng A1999; 267: 260-266.

207. McAlarney, Oshiro, and McAlarney, International Journal of Oral and Maxillofacial Implants 1996; 11: 73-80.
208. B. Groessner-Schreiber, and R. S. Tuan, J. Cell Sci.1992; 101: 209-217.
209. J. C. Keller, G. B. Schneider, C. M. Stanford, and B. Kellogg, Implant Dent 2003; 12: 175-181.
210. E. Krasicka-Cydzik, PL Patent 367556 (2003).
211. G. E. Thompson, and G. C. Wood, Nature 1981; 290: 230-232.
212. S. Iijima, Nature 1991; 354: 56-58.
213. M. Harada, and M. Adachi, Adv. Mater. 2000; 12: 839-841.
214. D. Gong, C. A. Grimes, O. K. Varghese, W. Hu, R. S. Singh, Z. Chen, and E.C. Dickey, J. Mater. Res. 2001; 16: 3331-3334.
215. P. Hoyer, Langmuir 1996; 12: 1411-1413.
216. Q. Zhang, L. Gao, J. Sun, and S. Zheng, Chem. Lett. 2002; 31: 226-227.
217. Q. Fan, B. McQuillin, D. D. C. Bradley, S. Whitelegg, and A. B. Seddon, Chem. Phys. Lett. 2001; 347: 325-330.
218. Z. Ma, Y. Yue, X. Deng, and Z. Gao, J. Mol. Catal. A 2002; 178: 97-104.
219. X-S. Ye, Z-G. Xiao, D-S. Lin, S-Y. Huang, and Y-H. Man, Mater. Sci. and Eng. B 2000; 74: 133-136.
220. A. Rothschild, F. Edelman, Y. Komem, and F. Cosandey, Sens. Actuators B 2000; 67: 282-289.
221. O. J. Whittemore, and J. J. Sipe, Powder Technol. 1974; 9: 159-164.
222. W. J. Lee, M. Alhoshan, and W. H. Smyrl, Journal of The Electrochemical Society 2006; 153(11): B499-B505.

223. O. K. Varghese, D. Gong, M. Paulose, C. A. Grimes, and E.C. Dickey, J. Mater. Res. 2003; 18: 156-165.

224. A. Ghicov, H. Tsuchiya, J. M. Macak, and P. Schmuki, Phys. Stat. Sol. (a) 2006; 203: R28-R30.

225. J. M. Macak, S. Aldabergerova, A. Ghicov, and P. Schmuki, Phys. Stat. Sol. (a) 2006; 203: R67-R69.

226. J. Zhao, X. Wang, T. Sun, and L. Li, Nanotechnology 2005; 16: 2450-2454.

227. J. M. Macak, H. Hildebrand, U. Marten-Jahns, and P. Schmuki, J. Electroanal. Chem. 2008; 621: 254-266.

228. S. P. Albu, D. Kim, and P. Schmuki, Angew. Chem. Int. Ed. 2008; 47: 1916-1919.

229. Q. Y. Cai, M. Paulose, O. K. Varghese, and C.A. Grimes, J. Mater. Res. 2005; 20: 230-236.

230. J. Zhao, X. Wang, R. Chen, and L. Li, Solid State Commun. 2005; 134: 705-710.

231. G. K. Mor, O. K. Varghese, M. Paulose, N. Mukherjee, and C. A. Grimes, J. Mater. Res. 2003; 18: 2588-2593.

232. ASM Handbook Committee, Metals Handbook-Corrosion of Metallic implants and Prosthetic Devices, vol. 13, ninth ed., American Society for Metals, Metals Park, 1987.

233. K. J. Bundy, Crit. Rev. Biomed. Eng. 1994; 22 (3/4): 139-251.

234. K. Bordji, J.Y. Jozeau, D. Mainard, E. Payar, P. Nether, T. Stucky, and M. age Ali, Biomaterials 1996; 17: 929-940.

235. Kitsugi, T. Nakayama, M. Oka, W. Q. Yan, T. Goto, T. Shibuya, T. Kokubo, and S. Miyaji, J Biomed Mater Res 1996; 32: 149-156.
236. M. Browne, J. Gregson, and R. H. West, J. Mater. Sci.: Mater. Med. 1996; 7: 323-329.
237. R. M. Pilliar, J. Biomed. Mater. Res. Appl. Biomater. 1987; 21:1-33.
238. R. M. Pilliar, Int J Powder Metal 1998; 34: 33-45.
239. C. A. Simmons, N. Valiquette, and R. M. Pilliar, J Biomed Mater Res 1999; 47: 127-138.
240. Y. Z. Yang, J. M. Tian, J. T. Tian, Z. Q. Chen, X. J. Deng, and D. H. Zhang, J Biomed Mater Res 2000; 52: 333-337.
241. L. D. Piveteau, B. Gasser, and L. Schlapbach, Biomaterials 2000; 21: 2193-2201.
242. T. Jinno, V. M. Goldberg, D. Davy, and S. Stevenson. J Biomed Mater Res 1998; 42: 20-29.
243. D. G. Kolman, and J. R. Scully, J. Electrochem. Soc. 1995; 142: 2179-2188.
244. E. M. Patrito, R. M. Torresi, E. P. M. Leiva, and V. A. Macagno, J. Electrochem. Soc.1990; 137: 524-530.
245. E. Kelly, in: J. O. M. Bockris, B. E. Conway, and R. White (Eds.), Modern Aspects of Electrochemistry, Plenum, New York, 1982; p 319.
246. J. Pan, D. Thierry, and C. Leygraf, Electrochim. Acta 1995; 41:1143-1153.
247. D. J. Blackwood, L. M. Peter, and D. E. Williams, Electrochim. Acta 1988 ; 33: 1143-1149.

248. S. Ferdjani, D. David, and G. Beranger, J. Alloys Compd. 1993; 200:191-194.

249. L. D. Arsov, C. Kormann, and W. Plieth, J. Electrochem. Soc. 1991; 138: 2964-2670.

250. C. P. De Pauli, M. C. Giordano, and J. O. Zerbino, Electrochim. Acta 1983; 28: 1781-1788.

251. S. H. Bonilla, and C. F. Zinola, Electrochim. Acta 1998; 43: 423-426.

252. D. J. Blackwood, and L. M. Peter, Electrochim. Acta 1989; 34: 1505-1511.

253. A. Müller, G. S. Popkirov, and R. N. Schindler, Ber. Bunsenges. Phys. Chem. 1992; 96: 1432-1437.

254. M. A. Abdel-Rahim, J. Appl. Electrochem. 1995; 25: 881-885.

255. M. Pourbaix, Atlas of Electrochemical Equilibria in Aqueous Solutions, ACE; Houston, 1974.

256. F. Di Quarto, S. Piazza, and C. Sunseri, Electrochim. Acta 1990; 35: 99-107.

257. S. R. Biaggio, N. Bocchi, R. C. Rocha-Filho, and F. E. Varela, J. Braz. Chem. Soc. 1997; 8: 615-620.

258. S. Kudelka, A. Michaelis, and J. W. Schultze, Electrochim. Acta1996; 41: 863-870.

259. S. Kudelka, and J. W. Schultze, Electrochim. Acta 1997; 42: 2817-2825.

260. O. R. Camara, C. P. De Pauli, and M. C. Giordano, Electrochim. Acta 1984; 29: 1111-1117.

261. M. M. Lohrengel, Electrochim. Acta 1994; 39: 1265-1271.

Publications

1. **Madhav Prasad Neupane**, Yu Kyoung Kim, Il Song Park, Min Ho Lee, Tae Sung Bae. Characterization of surface oxide films and cell toxicity evaluations with a quenched titanium surface. METALS AND MATERIALS International Vol. 14, No.4 (2008), pp. 443-448.
2. **Madhav Prasad Neupane**, Yu Kyoung Kim, Il Song Park, Sook Jeong Lee, Min Ho Lee and Tae Sung Bae. Effect of electrolyte pH on the structure and *in vitro* osteoblasts response to anodic titanium oxide. METALS AND MATERIALS International Vol. 14, No.5 (2008), pp. 607-613.
3. **Madhav Prasad Neupane**, Il Song Park, Min Ho Lee, Tae Sung Bae and FumioWatari. Influence of heat treatment on morphological changes of nano-structured titanium oxide formed by anodic oxidation of titanium in acidic fluoride solution. Bio-Medical Materials and Engineering Vol. 19, No. 1 (2009), pp. 77-83.
4. **Madhav Prasad Neupane**, Yu Kyoung Kim, Sook Jeong Lee, Il Song Park, Min Ho Lee, Kyoung A Kim, and Tae Sung Bae. Temperature driven morphological changes of hydrothermally prepared copper oxide nanoparticles. Surface and Interface Analysis Vol. 41, Issue 3 (2009), pp 259-263.

Conference Proceeding

1. **Madhav Prasad Neupane**, Min Ho Lee, Il Song Park and Tae Sung Bae. The influence of pH on the surface oxidation of titanium by anodic oxidation. 2006 Young Scientist Competition Symposium, Center for Health-Care Technology Development September 29, 2006, Jeonju, South Korea.
2. **Madhav Prasad Neupane**, Yu Kyoung Kim, Min Ho Lee, Il Song Park and Tae Sung Bae. Anodic oxidation of pure titanium metal using phosphate buffer solution. Symposium "Korea Research Society for Dental Materials" November 3, 2006, Suncheon, South Korea.
3. **Madhav Prasad Neupane**, Yu Kyoung Kim, Min Ho Lee, Il Song Park and Tae Sung Bae. Effect of electrolyte pH on the titanium oxide formation and osteoblast response *in vitro*. International Conference organized by Korean Institute of Metals and Materials April 27, 2007, Changwon, South Korea.
4. Tae Sung Bae, Min Ho Lee, R. S. Lee, **Madhav Prasad Neupane**, Sang Yong Won, Il Song Park and Jeong Mo Yoon. Evaluation of fatigue characterization of implant abutment combination. 21st IADR and 19th SEAADE Annual Science Meeting, Indonesia, Bali 2007, September 8.
5. **Madhav Prasad Neupane**, Yu Kyoung Kim, Il Song Park, Min Ho Lee, Tae Sung Bae. Characterization of surface oxide films and cell toxicity evaluation with quenched titanium surface. Symposium "Korea Research Society for Dental Materials" May 1, 2008.

6. **Madhav Prasad Neupane**, Il Song Park, Min Ho Lee, Tae Sung Bae and Fumio Watari. Fabrication and influence of heat treatment on nano-structured titanium oxide. International Symposium on "Nanotoxicology Assessment and Biomedical Environmental Application of Fine Particles and Nanotubes (ISNT 2008)", Hokkaido, Japan 2008, June 16-17.
7. Yu Kyoung Kim, Man Hyung Lee, **Madhav Prasad Neupane**, Il Song Park, Min Ho Lee, Kyeong Won Seol and Tae Sung Bae. Surface characteristics of magnesium alloys treated by anodic oxidation using pulse power. International Conference on Multifunctional Materials and Structures, Hong Kong 28-31 July, 2008.
8. **Madhav Prasad Neupane**, Yu Kyoung Kim, Il Song Park, Min Ho Lee, Tae Sung Bae, Mi Kyung Yu, Kwang Won Lee. Influence of the number of carboxyl groups on the nucleation of hydroxyapatite. 2008 Fall Conference of the Korean Institute of Metals and Materials, October 23-24, Incheon, Korea.

Acknowledgements

I would like to express the sincere gratitude to my advisor, Prof. Dr. Min Ho Lee, for giving me this great opportunity to further my education. Also, thanks go to him for all his powerful support and encouragement. I highly appreciate Prof. Dr. Tae Sung Bae for his valuable guidance and help. I would like to give special thanks to my co-workers Dr. Il Song Park, and Yu Kyoung Kim for their cooperation and assistance. Special gratitude is extended to Mrs. Eu Ri Lee who guided me in laboratory and especially helped me all biological work. Thanks to Man Hyung Lee for his valuable help in laboratory and characterization of materials and also thanks to Jang Gwon Bae for his co-operation in laboratory. Sincere acknowledgement is also expressed to my dear friend Dr. Santosh Aryal who showed a way to me in Korea and encouraged and guided me in research way, Dr. Remant Bahadur K. C. and Dr. Shanta Raj Bhattarai for their support and cooperation. Thanks to Mr. Madhab Prasad Bajgai, and Daman Chandra Parajuli who always support me in my research work as a members of same Bionanosystem Engineering Department. I would like to thank to my all well wishers Sushil, Subash, Rabindra, Gyanendra, Shiba, Bishow, Kishor, Govinda, Janardhan, Manoj, Pashupati, Dilip, Babu Kaji, Maheshwor, Deependra, Bidur, Amin, Geeta, Apshara, Bhawana, Prava, Shishir, and Subesh.

I couldn't resist without giving heartful thanks to my parents, family and relatives. Father Toya Nath Neupane and mother Guna Maya Neupane who sacrificed everything to make me a better person, who used get happy in my little success and encouraged me every steps of life. They are the most

influential person in my life who is always in the pursuit of the truth in everything. Also I would like to thank to my sisters Muna Neupane, Shanta Neupane, and Kopila Neupane, brother in laws Thakur Pant, Laxmi Kanta Gautam, and Prakash Dhakal. I am thankful for the admirable aspiration from father in law Tirtha Raj Poudel, mother in law Sita Poudel, sister Shrijana Poudel, Brother Santosh Poudel and Niroj Poudel.

At last it's my great pleasure to honor my wife Apshara with heartful thanks for the sprit of love and affection. The sacrifices, she has done to glow on me indeed is a great achievement of my life. I wish her love would inspire me to explore a bloomed and admired figure in our society. My beloved daughter Asma who alone lives in Nepal, sacrifices her childhood for my study. I am very much thankful to her.